# Mechanism of Bactericidal and Fungicidal Activities of Textiles Covalently Modified With Alkylated Polyethylenimine

**Jian Lin,[1] Shuyi Qiu,[1] Kim Lewis,[2] Alexander M. Klibanov[1]**

*[1]Department of Chemistry and Division of Biological Engineering, Massachusetts Institute of Technology, Cambridge, Massachusetts 02139; telephone: 617-253-3556; fax: 617-252-1609; e-mail: klibanov@mit.edu*
*[2]Department of Biology, Northeastern University, Boston, Massachusetts*

*Received 13 November 2002; accepted 16 December 2002*

*DOI: 10.1002/bit.10651*

**Abstract:** Our previous studies have led to a novel "non-release" approach to making materials bactericidal by covalently attaching certain moderately hydrophobic polycations to their surfaces. In the present work, this strategy is extended beyond the heretofore-used nonporous materials to include common woven textiles (cotton, wool, nylon, and polyester). Pieces of such cloths derivatized with *N*-hexylated+methylated high-molecular-weight polyethylenimine (PEI) are strongly bactericidal against several airborne Gram-positive and Gram-negative bacteria. In contrast, the immobilized and *N*-alkylated PEIs of low molecular weight have only a weak, if any, bactericidal activity. These findings support a mechanism of the antibacterial action whereby high-molecular-weight and hydrophobic polycationic chains penetrate bacterial cell membranes/walls and fatally damage them. The bactericidal textiles prepared herein are lethal not only to pathogenic bacteria but to fungi as well. © 2003 Wiley Periodicals, Inc. *Biotechnol Bioeng* **83**: 168–172, 2003.

**Keywords:** polycations; immobilization; microbicidal materials; fibers; cotton; molecular weight of polymers

against a variety of Gram-positive and Gram-negative bacteria, whether airborne or waterborne (Lin et al., 2002a, 2002b; Tiller et al., 2001, 2002). Thus far, however, this approach has been validated for only nonporous materials (Borman, 2002) and only against bacterial pathogens.

The defining mechanistic feature of the aforementioned strategy is that it is *not* based on a gradual release of an entrapped antiseptic agent (Tiller et al., 2001). Similar non-release claims have been made for antibacterial materials developed by other investigators (Borman, 2002; Isquith et al., 1972; www.microbeshield.com), whereby fatty alkyl groups were attached to surfaces via ammonium anchors. However, in contrast to our immobilized *polymers* (Lin et al., 2002a, 2002b; Tiller et al., 2001, 2002), it is difficult to imagine how these relatively short chains can fatally penetrate bacterial membranes and/or cell walls.

In the present investigation, we extend our bactericidal technology to textiles made of cotton, wool, nylon, or polyester. Moreover, such porous, woven materials bearing co-

## Titration of Primary and Quaternary Amino Groups

*Primary amino groups* (Lee and Loudon, 1979). A 2×2-cm wool cloth was immersed in 2 mL of a 0.1 *M* picric acidsolution in methylene chloride, followed by washing with 20 mL of the solvent, drying, and addition of 2 mL of dry *N*,*N*-diisopropylethylamine The density of the resultant NH2 groups was found to be 0.92 ± 0.02 nmol/cm2

*Quaternary amino groups* (Ledbetter and Bowen, 1969). A 2×2-cm alkyl-PEI-derivatized cloth was dipped in a 1% aqueous solution of fluorescein (Na salt), shaken for 5 min, thoroughly rinsed with distilled water, and placed in 20 mL of a 0.25% aqueous solution of cetyltrimethylammonium chloride. The densities of the quaternary amino groups on the *N*-alkylated PEI-derivatized cotton, wool, nylon, and polyester cloths were found to be 17.3 ± 0.4, 3.9 ± 0.8, 15.9 ± 0.8, and 9.1 ± 0.6 nmol/cm2, respectively.

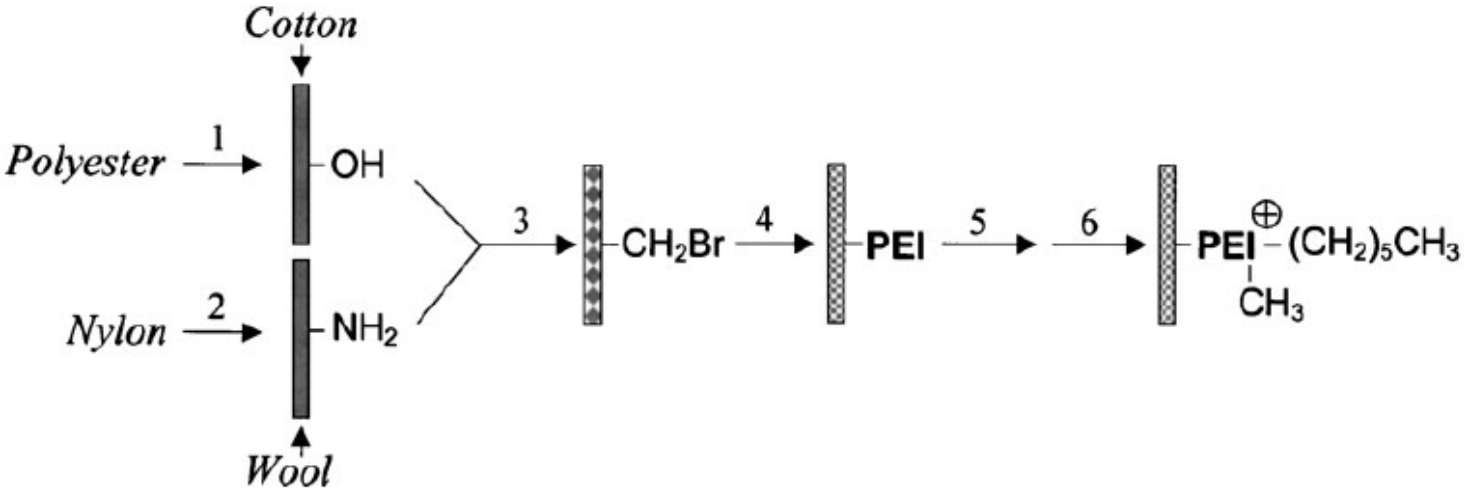


**Figure 1.** Schematic representation of the synthesis of *N*-alkylated PEIs covalently immobilized onto cotton, wool, nylon, or polyester cloths. Step 1: alkaline hydrolysis of polyester [poly(ethylene terephthalate)]; step 2: acid hydrolysis of nylon (Nylon-66); step 3: acylation of original or partially hydrolyzed textiles' hydroxyl or amino groups with 4-bromobutyryl chloride; step 4: covalent attachment (*N*-alkylation) of PEI; step 5: *N*-hexylation of the immobilized PEI with bromohexane; and step 6: *N*-methylation of the immobilized *N*-hexyl-PEI with iodomethane (see text).

**Table I.** Microbicidal efficiencies of four textiles derivatized with *N*-alkylated 750-kDa PEI against airborne bacteria and fungi.[a]

| | | Microbicidal activities (%)[b] | | | |
|---|---|---|---|---|---|
| Microorganism | Type | Cotton | Wool | Nylon | Polyester |
| *S. aureus* | Gram(+) | 98 ± 1 | 94 ± 2 | 96 ± 2 | 93 ± 1 |
| *S. epidermidis* | Gram(+) | 97 ± 1 | 98 ± 1 | 98 ± 1 | 97 ± 1 |
| *E. coli* | Gram(−) | 99 ± 1 | 98 ± 1 | 99 ± 1 | 96 ± 2 |
| *P. aeruginosa* | Gram(−) | 98 ± 1 | 97 ± 1 | 98 ± 1 | 98 ± 1 |
| *S. cerevisiae* | Fungus/yeast | 97 ± 1 | 98 ± 1 | 90 ± 2 | 88 ± 9 |
| *C. albicans* | Fungus/yeast | 96 ± 1 | 96 ± 3 | 91 ± 2 | 92 ± 7 |

[a]Immobilization and *N*-alkylation of PEI were carried out as outlined in Figure 1. For experimental details, see text.

[b]All measurements were done in duplicate with the mean values and standard errors obtained shown.

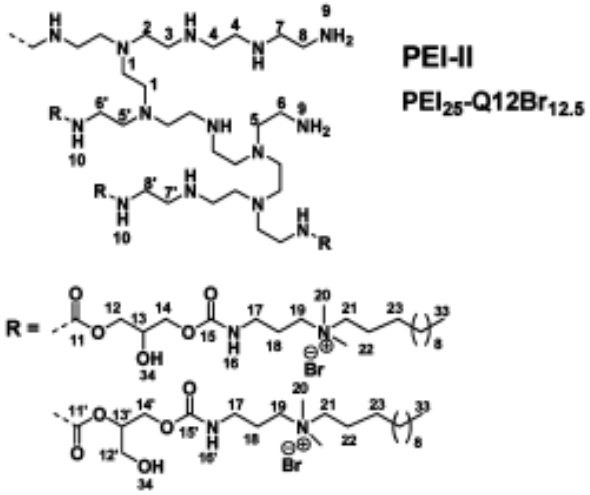

- Next, we explored whether the textiles with immobilized 750-kDa *N*-alkyl-PEI would be effective against airborne fungi. (Fungi/yeasts have a single membrane covered by a thick cell wall composed of glucan and chitin. This design is similar to the cell envelope of Gram-positive bacteria,composed of a membrane covered with a peptidoglycan wall. In Gram-negative bacteria, an additional outer membrane is found above the peptidoglycan wall [Lewis, 2001].)

**Table I.** Microbicidal efficiencies of four textiles derivatized with *N*-alkylated 750-kDa PEI against airborne bacteria and fungi.[a]

| Microorganism | Type | Microbicidal activities (%)[b] | | | |
|---|---|---|---|---|---|
| | | Cotton | Wool | Nylon | Polyester |
| *S. aureus* | Gram(+) | 98 ± 1 | 94 ± 2 | 96 ± 2 | 93 ± 1 |
| *S. epidermidis* | Gram(+) | 97 ± 1 | 98 ± 1 | 98 ± 1 | 97 ± 1 |
| *E. coli* | Gram(−) | 99 ± 1 | 98 ± 1 | 99 ± 1 | 96 ± 2 |
| *P. aeruginosa* | Gram(−) | 98 ± 1 | 97 ± 1 | 98 ± 1 | 98 ± 1 |
| *S. cerevisiae* | Fungus/yeast | 97 ± 1 | 98 ± 1 | 90 ± 2 | 88 ± 9 |
| *C. albicans* | Fungus/yeast | 96 ± 1 | 96 ± 3 | 91 ± 2 | 92 ± 7 |

[a]Immobilization and *N*-alkylation of PEI were carried out as outlined in Figure 1. For experimental details, see text.

[b]All measurements were done in duplicate with the mean values and standard errors obtained shown.

**Table II.** Bactericidal potencies against airborne *S. aureus* of cotton-immobilized and *N*-alkylated PEIs of different molecular weights as a function of washing.[a]

| Molecular weight of PEI (kDa) | Bactericidal activities (%) after: | | |
|---|---|---|---|
| | Regular wash[b] | First exhaustive wash[c] | Second exhaustive wash[c] |
| 750 | 98 ± 1 | 98 ± 1 | 95 ± 3 |
| 25 | 83 ± 3 | 75 ± 11 | 70 ± 6 |
| 2 | 53 ± 17 | 35 ± 15 | 37 ± 8 |
| 0.8 | 58 ± 10 | 24 ± 4 | 19 ± 13 |

[a]See footnotes to Table I.

[b]Consisted of washing with methanol and distilled water.

[c]Consisted of additional stirring in soapy water at 55°C overnight, followed by thorough rinsing with distilled water.

One can see that neither the first nor the second cycle had any appreciable effect on the bactericidal potency of the cottonimmobilized and *N*-alkylated 750-kDa PEI (first row in Table II). (Likewise, this exhaustive washing of the *N*alkylated high-molecular-weight PEI immobilized onto wool, nylon, and polyester did not noticeably diminish the bactericidal potency.) In contrast, this washing substantially cut the bactericidal efficiencies of the immobilized and *N*alkylated PEIs of smaller sizes.

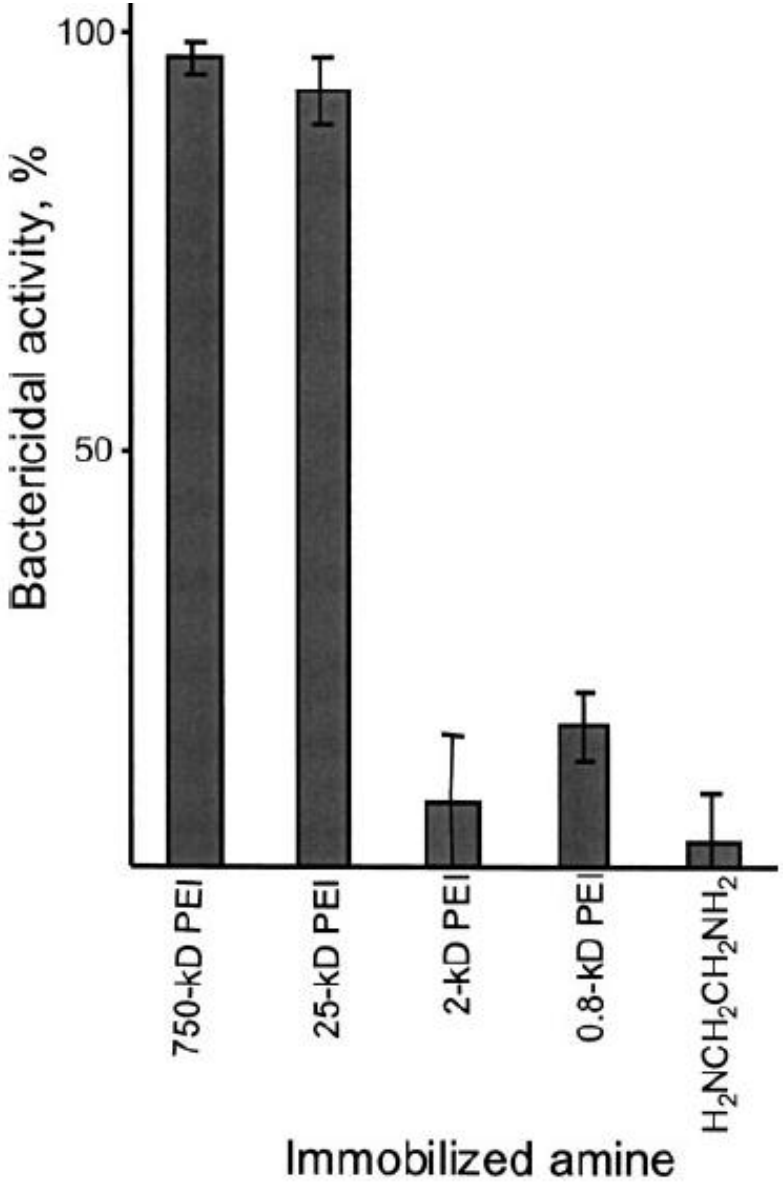


**Figure 2.** Bactericidal activities against airborne *S. aureus* of the *N*-alkylated PEIs of different molecular weights, as well as of 1,2-diaminoethane, covalently attached (as in Fig. 1) to $NH_2$-glass slides (see text).

It should be emphasized that fatty alkyl chains attached to surfaces through quaternary amine anchors in the reported alternative antibacterial materials (Borman, 2002; Isquith et al., 1972; www.microbeshield.com) are far shorter than even the 0.8-kDa PEI. Therefore, such materials *cannot* function via the same “hole-poking” mechanism as described in this study and elsewhere (Lin et al., 2002a, 2002b; Morgan et al., 2000; Tiller et al., 2001, 2002).

Biomacromolecules

ARTICLE

pubs.acs.org/Biomac

# Recyclable Antibacterial Magnetic Nanoparticles Grafted with Quaternized Poly(2-(dimethylamino)ethyl methacrylate) Brushes

Hongchen Dong,[†] Jinyu Huang,[‡] Richard R. Koepsel,[§] Penglin Ye,[†] Alan J. Russell,[*,§] and Krzysztof Matyjaszewski[*,†]

[†]Carnegie Mellon University, Chemistry Department, Pittsburgh, Pennsylvania 15213, United States

[‡]CIBA Vision Corporation, 11460 Johns Creek Parkway, Duluth, Georgia 30097, United States

[§]Department of Surgery and McGowan Institute for Regenerative Medicine, University of Pittsburgh, Suite 300, 450 Technology Drive, Pittsburgh, Pennsylvania 15219, United States

**ABSTRACT:** Highly efficient recyclable antibacterial magnetite nanoparticles consisting of a magnetic $Fe_3O_4$ core with an antibacterial poly(quaternary ammonium) (PQA) coating were prepared in an efficient four-step process. The synthetic pathway included: (1) preparation of $Fe_3O_4$ nanoparticles via coprecipitation of $Fe^{2+}/Fe^{3+}$ in the presence of an alkaline solution; (2) attachment of an ATRP initiating functionality to the surface of the nanoparticles; (3) surface-initiated atom transfer radical polymerization (ATRP) of 2-(dimethylamino)ethyl methacrylate (DMAEMA); and (4) transformation of PDMAEMA brushes to PQA via quaternization with ethyl bromide. The success of the surface functionalization was confirmed by FT-IR, thermal gravimetric analysis (TGA), elemental analysis, and transmission electron microscopy (TEM). The PQA-modified magnetite nanoparticles were dispersed in water and exhibited a response to an external magnetic field, making the nanoparticles easy to remove from water after antibacterial tests. The PQA-modified magnetite nanoparticles retained 100% biocidal efficiency against *E. coli* ($10^5$ to $10^6$ *E. coli*/mg nanoparticles) during eight exposure/collect/recycle procedures without washing with any solvents or water.

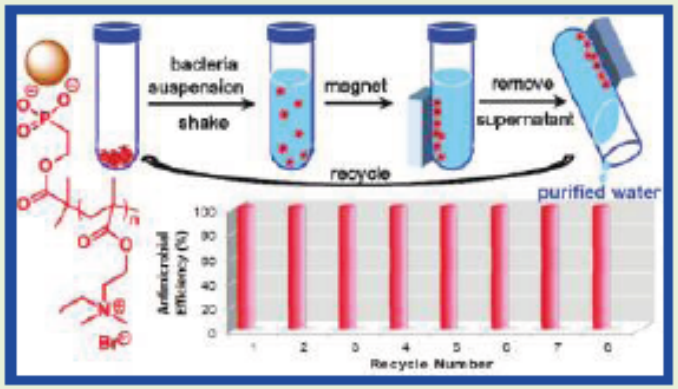

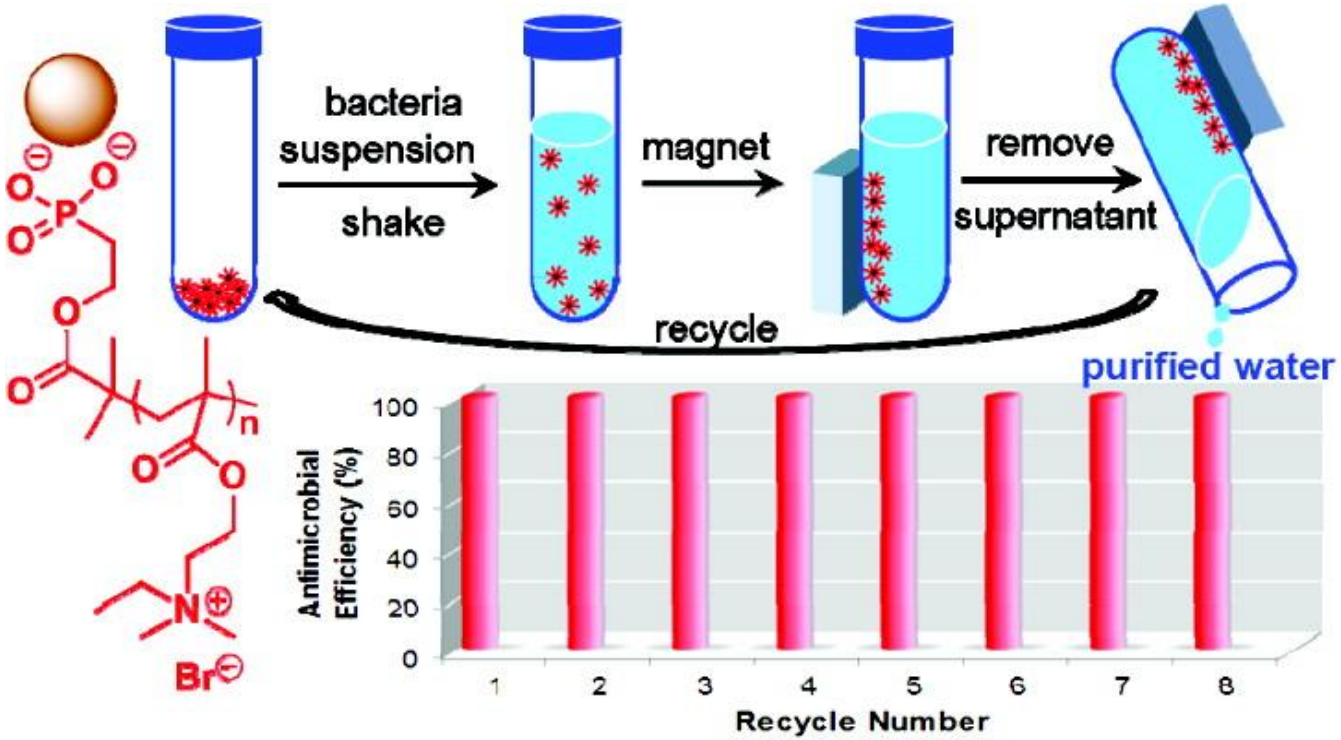

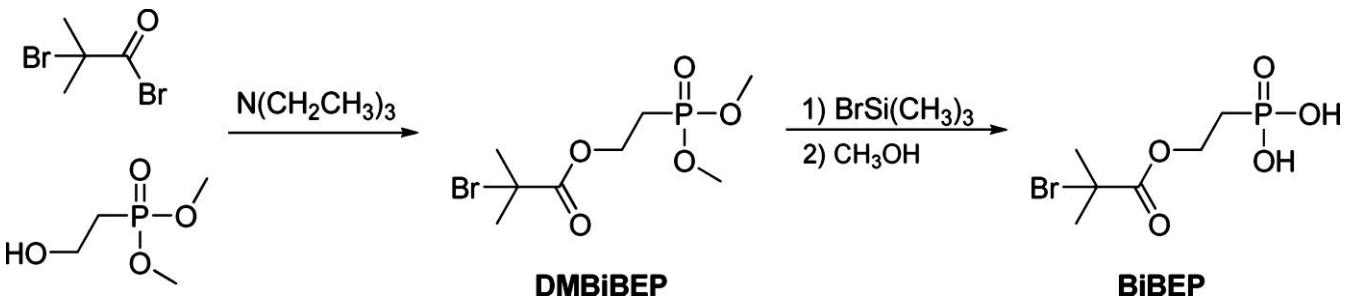


**DMBiBEP** **BiBEP**



Published in: Hongchen Dong; Jinyu Huang; Richard R. Koepsel; Penglin Ye; Alan J. Russell; Krzysztof Matyjaszewski; *Biomacromolecules* **2011,** 12, 1305-1311.

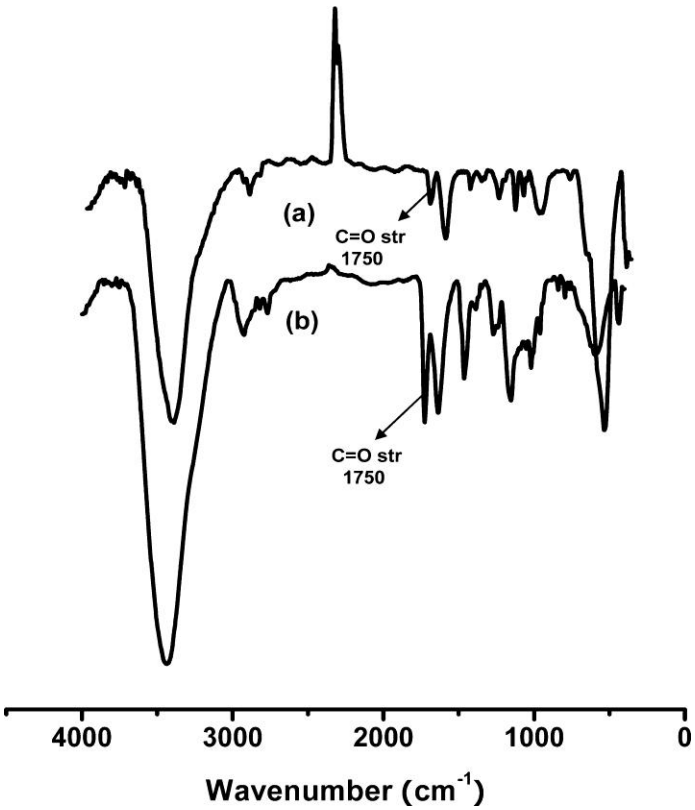


FT-IR spectra of magnetite nanoparticles (a) grafted with ATRP initiator BiBEP and (b) grafted with PDMAEMA.

A characteristic C=O stretch vibration band(1750 cm-1) was clearly observed in the IR spectrum of the modified magnetite nanoparticles.



Published in: Hongchen Dong; Jinyu Huang; Richard R. Koepsel; Penglin Ye; Alan J. Russell; Krzysztof Matyjaszewski; *Biomacromolecules* **2011,** 12, 1305-1311.

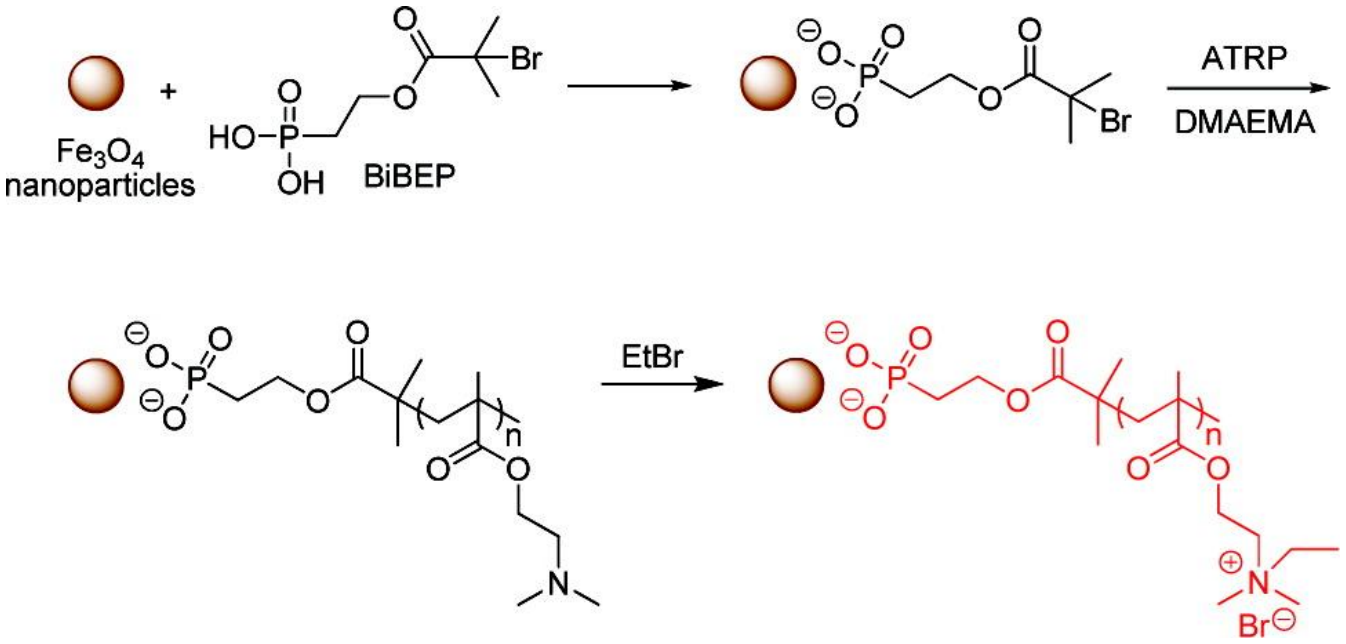

**Table 1. PDMAEMA-Modified Magnetite Nanoparticle**[a]

| entry | $[I]_0/[M]_0/[CuCl]_0/[CuCl_2]_0/[L]_0$[b] | $M_n$ (GPC) | $M_w/M_n$ (GPC) | organic mass (%) (TGA) | organic mass (%) (EA) |
|---|---|---|---|---|---|
| 1 | initiators only | | | 10 | 12 |
| 2 | 1:1570:4.1:0.8:5 | 10 700 | 1.6 | 55 | 50 |
| 3 | 1:1570:4.1:0.8:5 | 44 700 | 1.2 | 61 | 58 |
| 4 | 1:1570:8.2:1.7:10 | 152 100 | 2.1 | 93 | 88 |

[a] GPC: gel permeation chromatography; TGA: thermal gravimetric analysis; EA: elemental analysis. [b] M = DMAEMA; L = HMTETA; $[DMAEMA]_0$ = 5.5 M; solvent: acetone. Polymerization was carried out at 40 °C.

To determine the molecular weight of the tethered chains the magnetite core was etched with hydrochloric acid, and the cleaved polymer chains were characterizedusing GPC.Determination of the Amount of Quaternary Amines on MagnetiteNanoparticles. The density of quaternary ammonium groups onmagnetite nanoparticles was measured as the amount of fluorescein boundper gram of particles. Fluorescein staining of PQA-modified magnetite nanoparticles (Table 1, entry 3) showed that the solvent-accessible densityof quaternary ammonium groups on magnetite nanoparticles was $4.8 \ 10^{19}$/g particles.

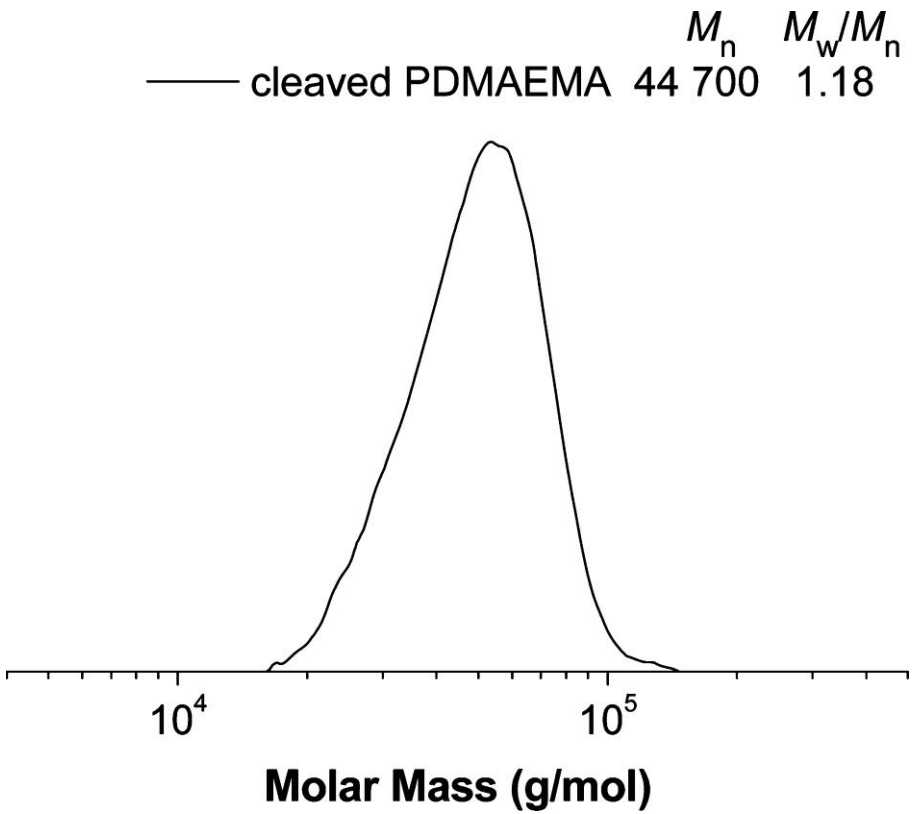


GPC trace of cleaved PDMAEMA chains (Table 1, entry 3).

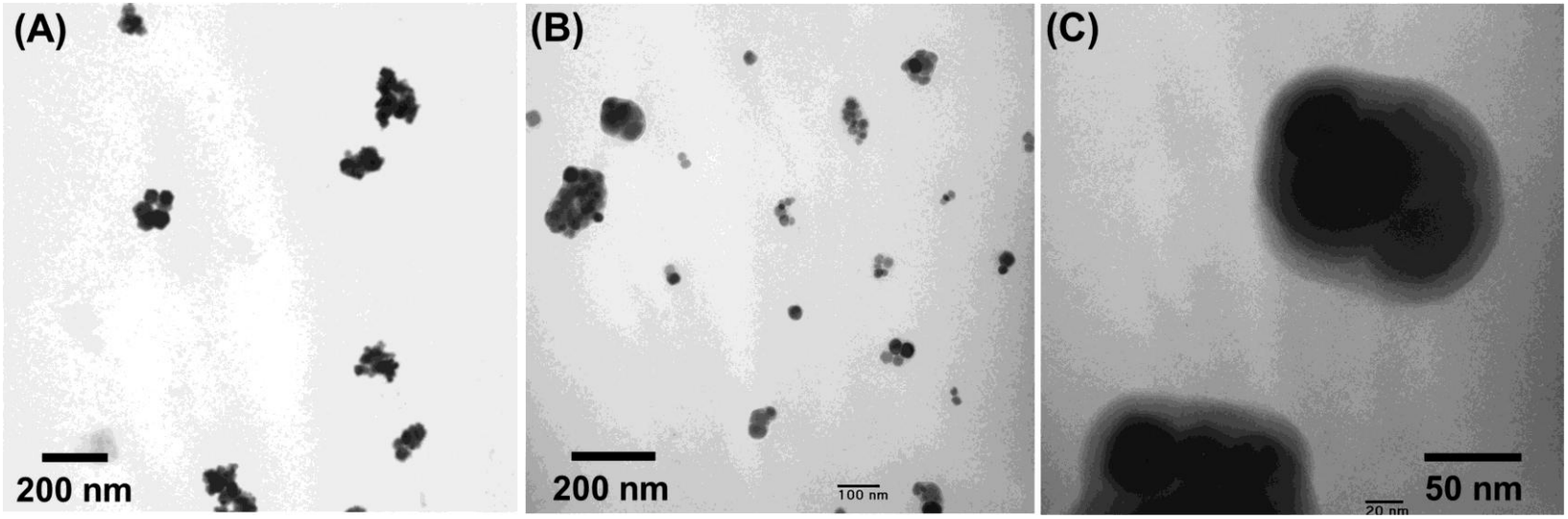


TEM images of (A) the initiator-modified and (B,C) PDMAEMA-grafted magnetite particles (Table 1, entry 3).

The particles described in Table 1, entry 3 were selected for their narrow size range and consistent coating thickness (Figure 3B,C) and for their ready dispersibility in water and toluene and were used for the functional testing.


Published in: Hongchen Dong; Jinyu Huang; Richard R. Koepsel; Penglin Ye; Alan J. Russell; Krzysztof Matyjaszewski; *Biomacromolecules* **2011,** 12, 1305-1311.

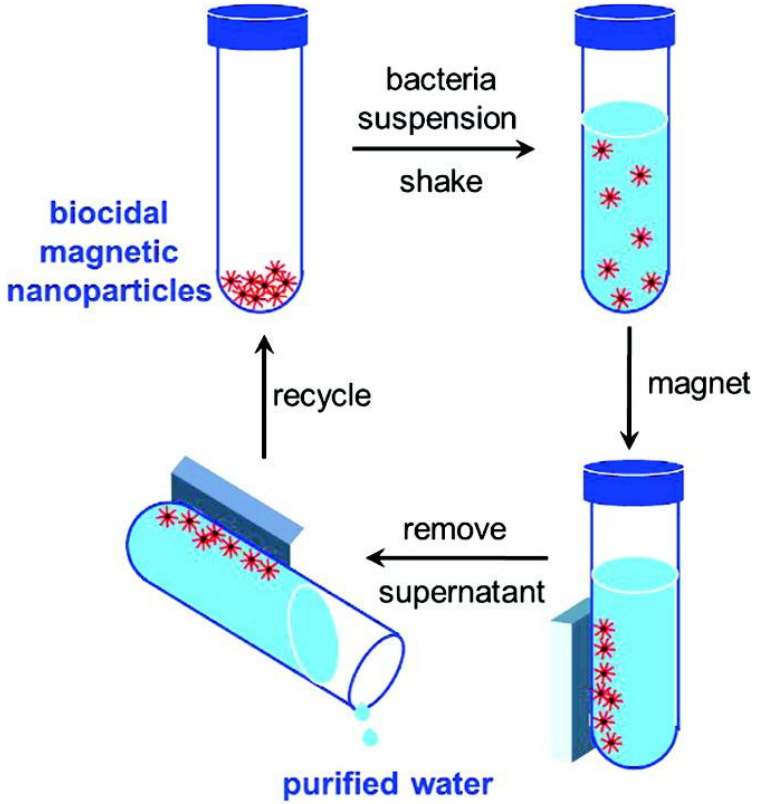


After exposure to an external magnetic field for 20 min, the majority of the nanoparticles were attracted to the source of the magnetic field. However, there was a small portion of magnetite nanoparticles remaining in the supernatant, which could be due to the low mass fraction of magnetite in these hybrid particles.


Published in: Hongchen Dong; Jinyu Huang; Richard R. Koepsel; Penglin Ye; Alan J. Russell; Krzysztof Matyjaszewski; *Biomacromolecules* **2011,** 12, 1305-1311.

**Table 2. Antimicrobial Activity of PQA-Modified Magnetic Nanoparticles[a]**

| | number of survived *E. coli*/mL | | | antimicrobial efficiency |
|---|---|---|---|---|
| | control[b] | PQA-modified magnetite no. 1[c] | PQA-modified magnetite no. 2[c] | |
| 1st cycle | $2.5 \times 10^5$ | 0 | 0 | 100% |
| 2nd cycle | $2.7 \times 10^5$ | 0 | 0 | 100% |
| 3rd cycle | $3.6 \times 10^5$ | 0 | 0 | 100% |
| 4th cycle | $4.0 \times 10^5$ | 0 | 0 | 100% |
| 5th cycle | $6.9 \times 10^5$ | 0 | 0 | 100% |
| 6th cycle | $6.1 \times 10^5$ | 0 | 0 | 100% |
| 7th cycle | $2.5 \times 10^5$ | 0 | 0 | 100% |
| 8th cycle | $2.8 \times 10^5$ | 0 | 0 | 100% |

[a] Concentration of PQA-modified magnetite particles = 1 mg/mL. [b] Control: bare magnetite particles (1 mg/mL). [c] PQA-modified magnetite nos. 1 and 2 are identical (Table 1, entry 3).

we separated the PQA-modified nanoparticles into two parts based on the response time to an external magnet. One required <10 min and the other needed >10 min.

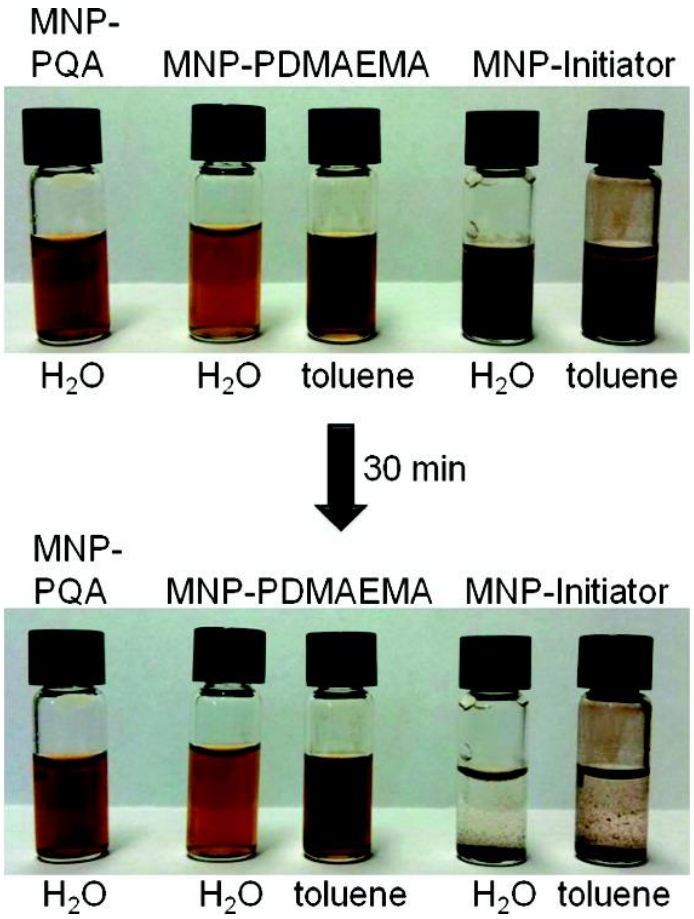


Stability of the suspensions of initiator, PDMAEMA, and PQA-modified nanoparticles in water and toluene (0.5 wt % of nanoparticles, Table 1, entry 3).

The aqueous suspensions of PQA- and PDMAEMA-modified magnetite nanoparticles as well as the toluene suspension of PDMAEMA-modified particles with up to 2 wt % of the nanoparticles remained stable for several months without sedimentation. In contrast, the initiator-modified magnetite nanoparticles precipitated shortly after being dispersed in either solvent.


Published in: Hongchen Dong; Jinyu Huang; Richard R. Koepsel; Penglin Ye; Alan J. Russell; Krzysztof Matyjaszewski; *Biomacromolecules* **2011,** 12, 1305-1311.


Images of PQA-modified nanoparticles (Table 1, entry 3) in water (2 mg/mL) (a) prior to and (b) after exposure to a permanent magnet for 10 min.


Published in: Hongchen Dong; Jinyu Huang; Richard R. Koepsel; Penglin Ye; Alan J. Russell; Krzysztof Matyjaszewski; *Biomacromolecules* **2011,** 12, 1305-1311.

# Permanent, Nonleaching Antibacterial Surfaces. 1. Synthesis by Atom Transfer Radical Polymerization

Sang Beom Lee,[†] Richard R. Koepsel,[‡] Scott W. Morley,[†] Krzysztof Matyjaszewski,[||] Yujie Sun,[§] and Alan J. Russell*[,†,‡,⊥]

*Department of Bioengineering, Department of Chemical and Petroleum Engineering, and Department of Chemistry, University of Pittsburgh, Pittsburgh, Pennsylvania 15260, Department of Surgery, McGowan Institute for Regenerative Medicine, Suite 200, 100 Technology Drive, Pittsburgh, Pennsylvania 15219, and Center for Macromolecular Engineering, Department of Chemistry, 4400 Fifth Avenue, Carnegie Mellon University, Pittsburgh, Pennsylvania 15213*

*Received September 12, 2003; Revised Manuscript Received January 23, 2004*

We have grown an antimicrobial polymer directly on the surfaces of glass and paper using atom transfer radical polymerization (ATRP). The method described here results in potentially permanent nonleaching antibacterial surfaces without the need to chemically graft the antimicrobial material to the substratum. The tertiary amine 2-(dimethylamino)ethyl methacrylate was polymerized directly onto Whatman #1 filter paper or glass slides via atom transfer radical polymerization. Following the polymerization, the tertiary amino groups were quaternized using an alkyl halide to produce a large concentration of quaternary ammonium groups on the polymer-modified surfaces. Incubating the modified materials with either *Escherichia coli* or *Bacillus subtilis* demonstrated that the modified surfaces had substantial antimicrobial capacity. The permanence of the antimicrobial activity was demonstrated through repeated use of a modified glass without significant loss of activity. Quaternary amines are believed to cause cell death by disrupting cell membranes allowing release of the intracellular contents. Atomic force microscopic imaging of cells on modified glass surfaces supports this hypothesis.

**Permanent, Nonleaching Antibacterial Surfaces. 1. Synthesis by Atom Transfer Radical Polymerization; Sang Beom Lee,Richard R. Koepsel,Scott W. Morley,Krzysztof Matyjaszewski, Yujie Sun,and Alan J. Russell,** *Biomacromolecules*, **2004**, *5* (3), pp 877–882
**DOI:** 10.1021/bm034352k
Publication Date (Web): February 27, 2004

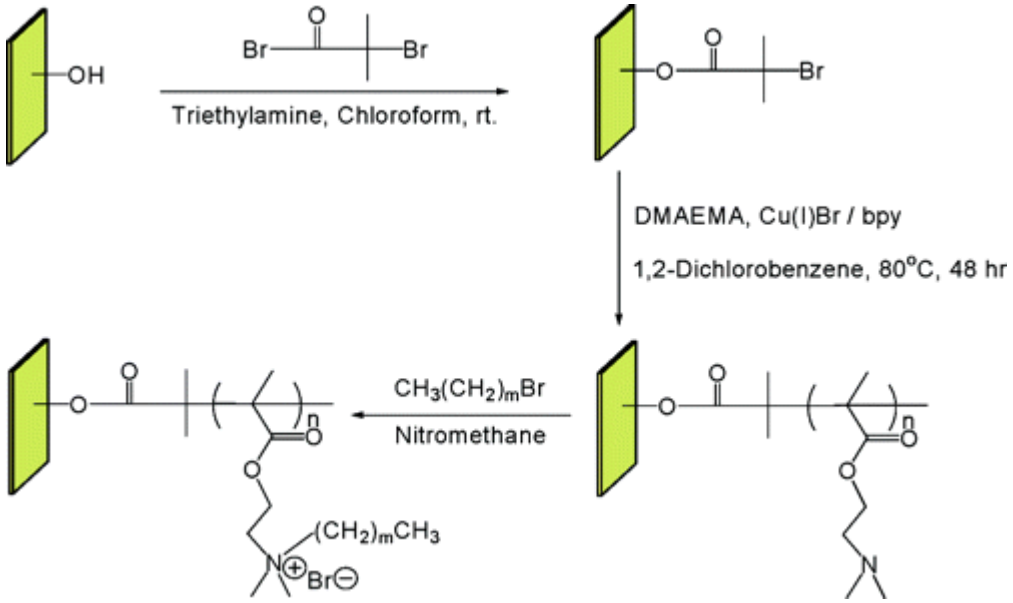

**Scheme 2**

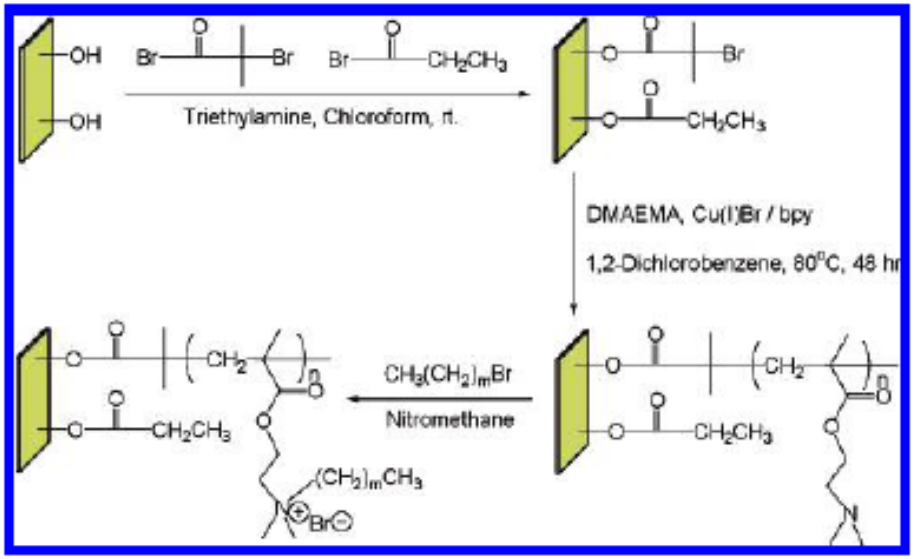


In some experiments, a “blocking agent” was used to synthesize filter papers with varying surfaces densities of the polymer as shown in Scheme 2. The propionyl bromide reacts with the hydroxyl groups found on the filter paper to produce a nonpolymerizable site.

Table 1. Results from GPC after Hydrolysis

| percent of initiator on surface | $M_n$/g mol$^{-1}$ | PDI |
|---|---|---|
| 100 | 21 100 | 2.22 |
| 100[a] | 21 900 | 1.62 |
| 50 | 23 000 | 2.21 |
| 10 | 19 300 | 2.14 |

[a] In the presence of sacrificial initiator.

To determine the molecular weight of the polymers synthesized by this method, papers were prepared with different initiator densities, and the completed polymer chains were cleaved from the surface by HCl hydrolysis. The GPC data for these experiments, presented in Table 1, show that the extent of the polymerization, and thus the length of the polymer chains, and the polydispersity index (PDI) are not greatly influenced by the number of initiation sites.

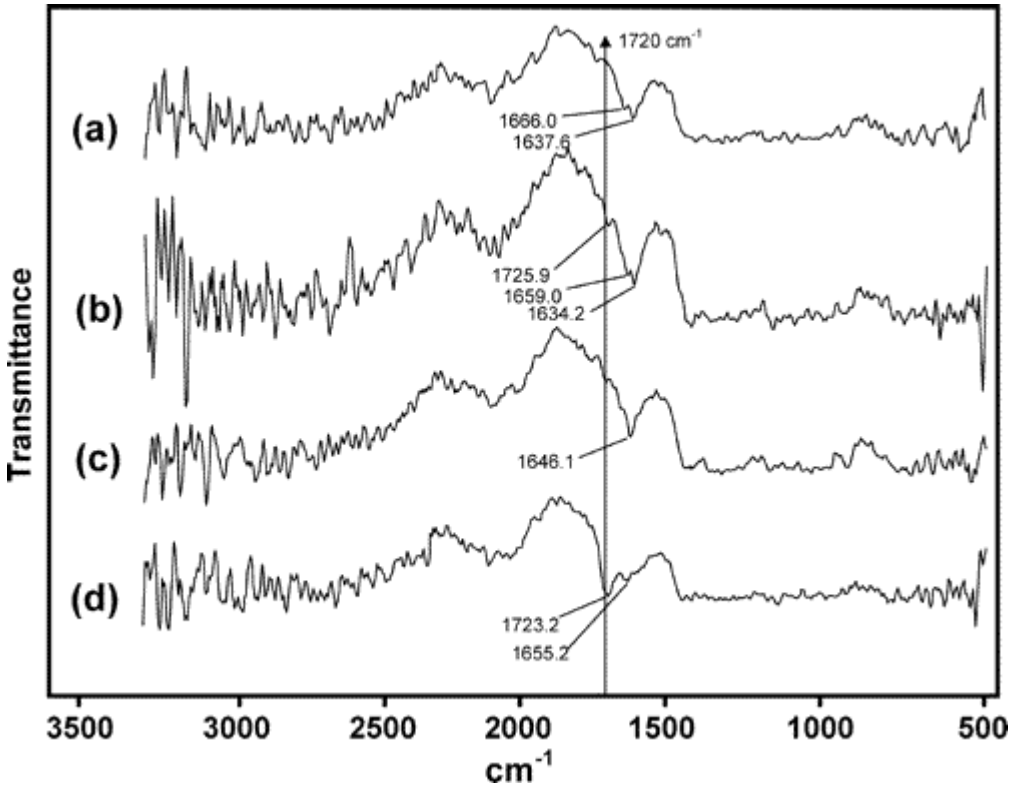


Figure 1 FT-IR of the grafted and ungrafted papers: pure paper (a); pure paper in the presence of sacrificial initiator (b); initiator-modified paper (c); and PDMAEMA-modified paper (d).

A carbonyl peak at 1720 cm-1 is a positive indicator for the poly(2-(dimethylamino)ethyl methacrylate) (PDMAEMA). This carbonyl peak is clearly seen on the grafted paper (Figure 1D) but not on pure paper (Figure 1A) or paper modified with initiator but not subjected to ATRP (Figure 1C).

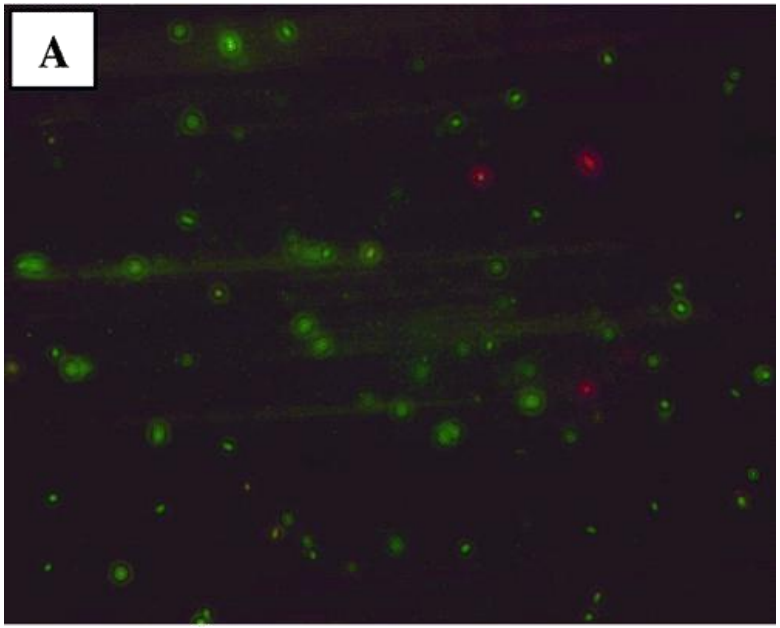


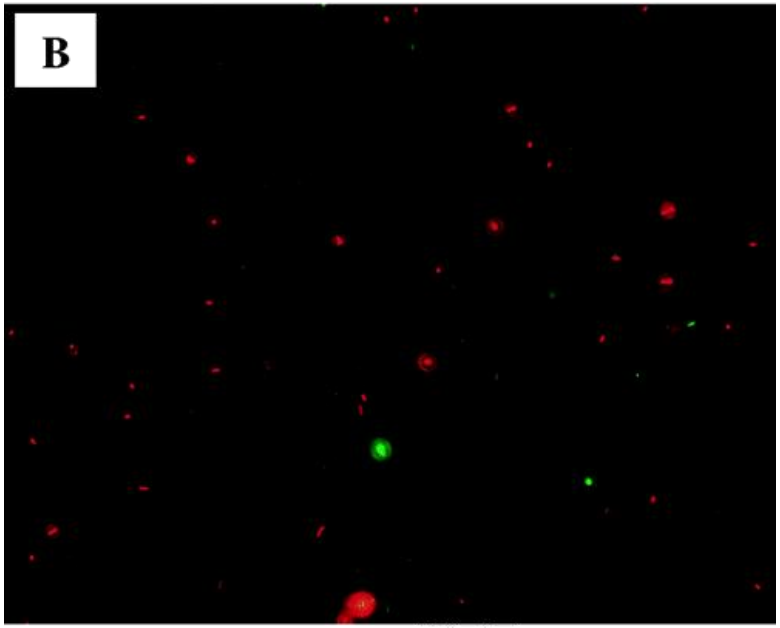


Figure 2 Live/dead analysis of *E. coli* incubated with papers. Panel A. cells incubated with nonmodified paper for 15 min. Panel B. Cells incubated with modified paper for 15 min

The lack of a zone of growth inhibition around any of the paper dots indicated that the material was not diffusing out of the paper. Since the material hydrolyzed from the paper (see Table 1) was no larger that 23 000 Da we believe that we are not washing loose polymer from the paper but are, rather, generating microfibers and small paper pieces with polymer attached to them. Treated glass slides did not release antimicrobialactivity into the buffer when shaken under experimental conditions

Interestingly, when the glass was washed with pure water, the antimicrobial activity disappears after two rounds of exposure to bacteria. Glass washed with SDS retains its antimicrobial activity. Washing the inactivated glass withdetergent resulted in the antimicrobial capacity returning to its original level. It is likely that material from the dead  Cells accumulates on the surface of the glass through a hydrophobic interaction. That  material is then removed by thedetergent with the concomitant restoration of the antimicrobialactivity of the surface. This result agrees with the notion that the mechanism of action of quaternary ammonium involves disruption of the plasma membrane causing the release of intracellular material.

**Table 2.** Antimicrobial Activity of Modified Paper and Glass[a]

| treated sample[b] | organism | number of bacteria added to sample | number of bacteria remaining |
|---|---|---|---|
| paper | *E. coli* | $2.6 \times 10^8$ | 0 |
| paper | *E. coli* | $1.6 \times 10^9$ | $4.9 \times 10^5$ |
| paper | *B. subtilis* | $6.2 \times 10^6$ | $6.0 \times 10^2$ |
| paper | *B. subtilis* spores | $2.5 \times 10^6$ | $1.3 \times 10^6$ |
| glass | *E. coli* | $9.4 \times 10^6$ | $1.4 \times 10^4$ |
| glass | *B. subtilis* | $1.0 \times 10^4$ | 0 |

[a] Samples were incubated with the number of bacteria as indicated. Following incubation the number of viable cells was determined by serial dilution. [b] All samples tested were compared to an untreated control of the same material.

Even though some cells survived, it should be noted that the paper was still extremely effective, killing a total of more than $10^9$ cells within 1 h. It should be noted that because paper is a fibrous material it has a much larger surface area than a piece of glass with the same dimensions. Because of this, a lower number of cells was incubated with the samples (Table 2). Glass samples were tested for their ability to kill *E. coli* and *B. subtilis* vegetative cells. The treated glass killed >9 $10^6$ *E. coli* and > 1 $10^4$ *B. subtilis*.

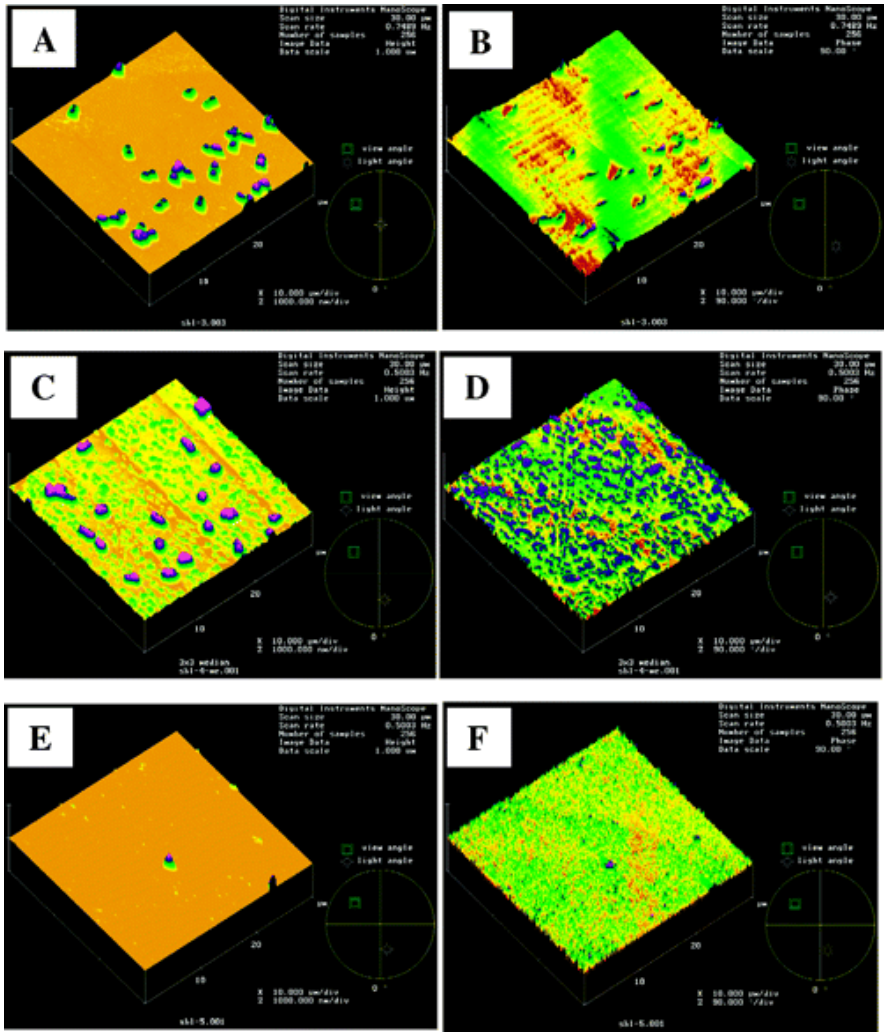


Figure 3 AFM images of glass surfaces. The pictures are: *E. coli* cells on plain glass A and B; *E. coli* cells on quaternized glass C and D; and quaternized glass without added cells E and F. Two data modes are shown for each location, height mode (A, C, and E) and the phase lag mode (B, D, and F). For the height mode, orange is the base color and represents the substrate surface. Relative height progresses through the spectrum with purple indicating the tallest structure. For the phase lag mode, orange represents the largest attraction between the tip and the substrate and purple is the weakest interaction

Quaternary amines are believed to cause cell death by disrupting cell membranes allowing release of the intracellular contents. Atomic force microscopic imaging of cells on modified glass surfaces supports this hypothesis. Perhaps the most interesting result comes from comparison of C and D. Thegreen spots in height mode that indicate the presence of material on the surface have become purple spots in phase lag mode. The fact that the material deposited on the surface has the same lack of attraction to the tip as the intact bacteria suggests that this material is of bacterial origin.

# Antibacterial Polypropylene via Surface-Initiated Atom Transfer Radical Polymerization

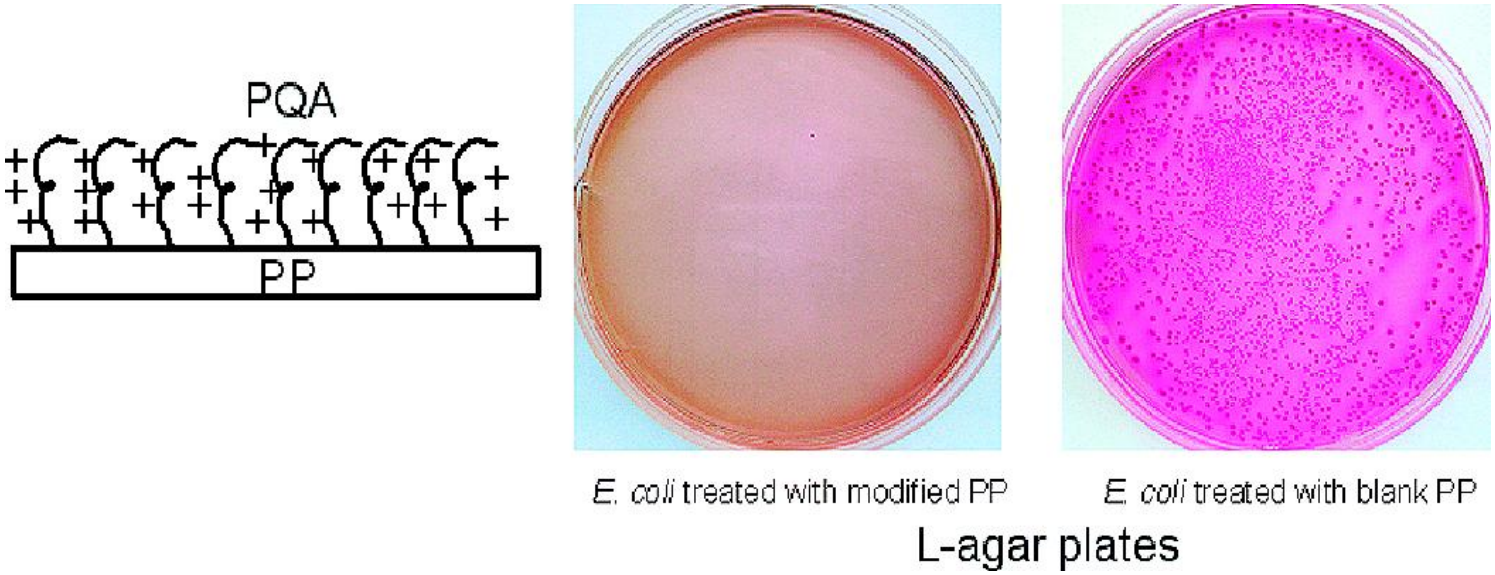


Jinyu Huang,[†] Hironobu Murata,[§] Richard R. Koepsel,[‡] Alan J. Russell,[*] and Krzysztof Matyjaszewski[*†]

Department of Chemistry, Carnegie Mellon University, Pittsburgh, Pennsylvania 15213, and Departments of Chemical and Petroleum Engineering, Bioengineering, and Surgery, McGowan Institute for Regenerative Medicine, Suite 200, 100 Technology Drive, Pittsburgh, Pennsylvania 15219

*Biomacromolecules*, 2007, 8 (5), pp 1396–1399

**DOI:** 10.1021/bm061236j

Publication Date (Web): April 7, 2007

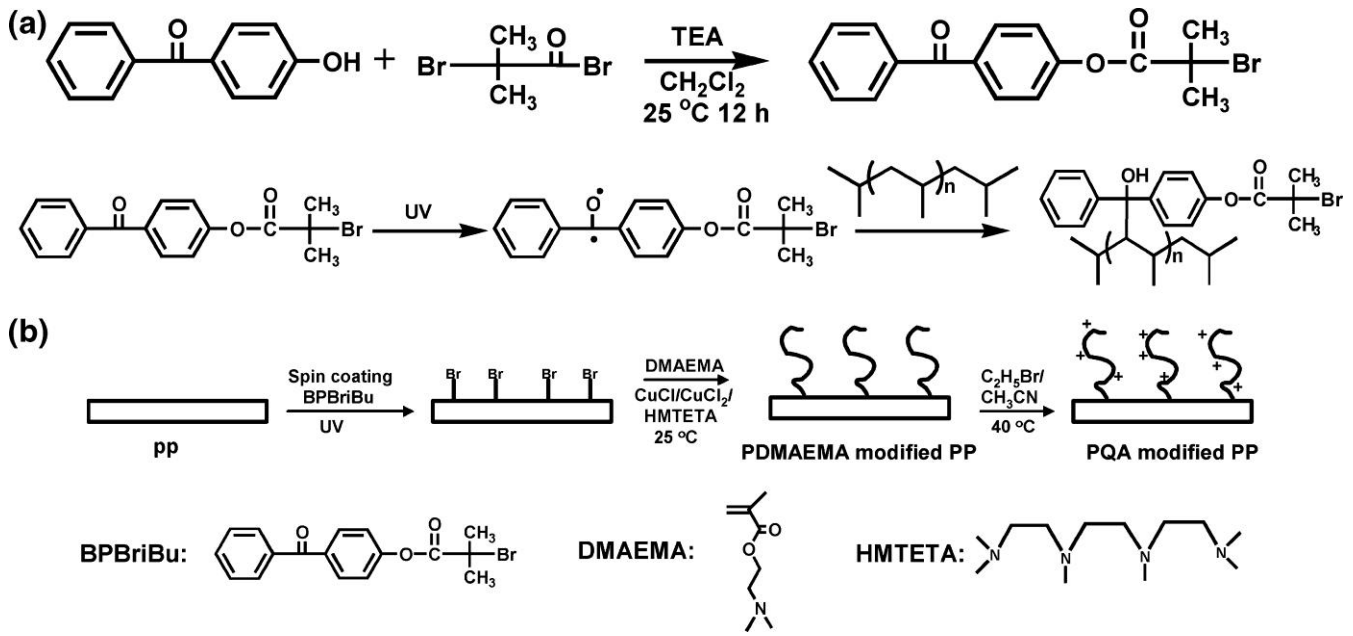


Scheme 1. Synthesis of 2-Benzophenonyl bromoisobutyrate and Benzophenone Chemistry (a) and a Schematic Drawing of Surface-Initiated ATRP of DMAEMA (b)

Published in: Jinyu Huang; Hironobu Murata; Richard R. Koepsel; Alan J. Russell; Krzysztof Matyjaszewski; *Biomacromolecules* **2007,** 8, 1396-1399.
DOI: 10.1021/bm061236j

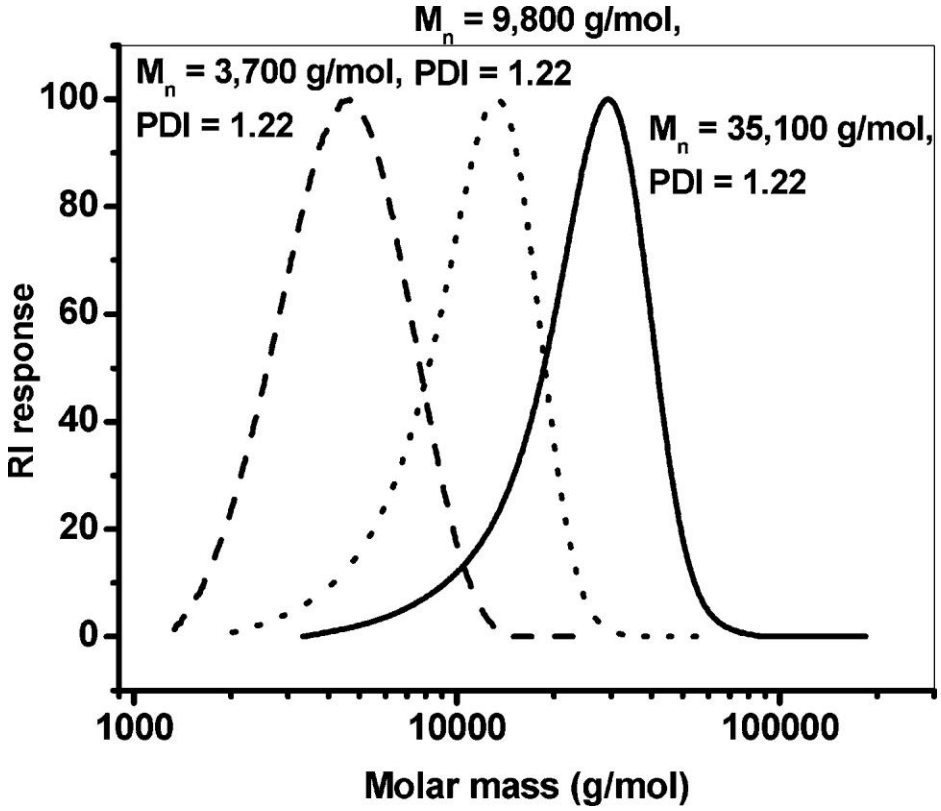


Figure 1 ATRP of DMAEMA initiated from the PP surface. [EBriBu]/[DMAEMA]/[CuCl]/[CuCl2]/[HMTETA] = 1:400:4:0.8:4.8; *V*monomer/*V*acetone = 4:1; *T* = 25 ° C.

Published in: Jinyu Huang; Hironobu Murata; Richard R. Koepsel; Alan J. Russell; Krzysztof Matyjaszewski; *Biomacromolecules* **2007,** 8, 1396-1399.
DOI: 10.1021/bm061236j

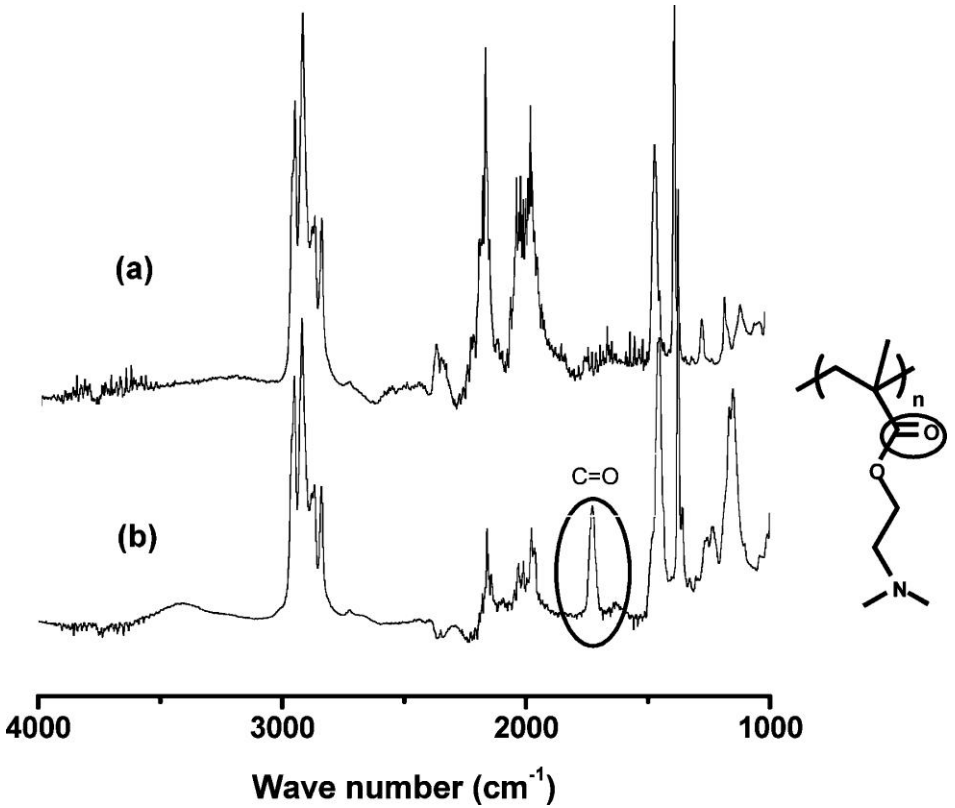


Figure 2 ATR-FTIR spectra of (a) untreated PP and (b) PP modified with PDMAEMA. (*M*n = 35,100 g/mol).

Published in: Jinyu Huang; Hironobu Murata; Richard R. Koepsel; Alan J. Russell; Krzysztof Matyjaszewski; *Biomacromolecules* **2007,** 8, 1396-1399.
DOI: 10.1021/bm061236j

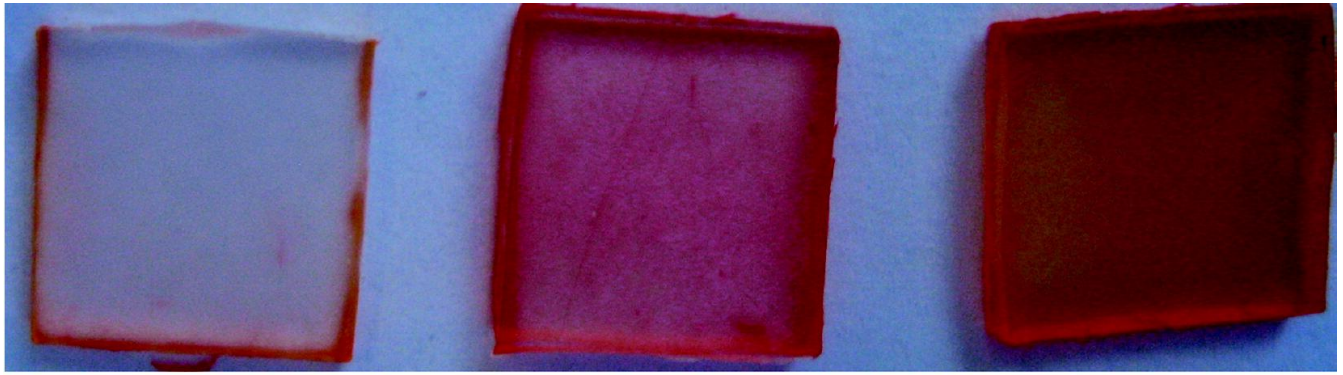


Figure 3 Digital pictures of the PP plates stained with fluorescein salt dye. (a) PP modified with PDMAMEA (*M*n = 1,500 g/mol); (b) PP modified with PDMAMEA (*M*n = 9,800 g/mol); (c) PP modified with PDMAMEA (*M*n = 21,300 g/mol).

Published in: Jinyu Huang; Hironobu Murata; Richard R. Koepsel; Alan J. Russell; Krzysztof Matyjaszewski; *Biomacromolecules* **2007,** 8, 1396-1399.
DOI: 10.1021/bm061236j

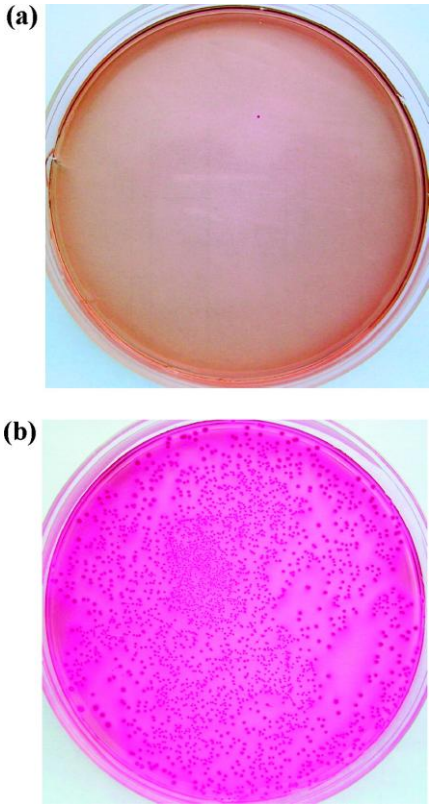


Figure 4 Photographs of l-agar plates onto which the *E. coli* suspension of distilled water treated with the PP slide (entry 3, Table 1) grafted with PQA (a) and the untreated PP slide (b) were deposited and incubated for 24 h. The PP slides were shaken with 5 mL of bacterial suspension for 1 h at 37 ˚ C. The solution was taken, diluted appropriately, and plated on l-agar plates. After overnight incubation, pictures were taken.

Published in: Jinyu Huang; Hironobu Murata; Richard R. Koepsel; Alan J. Russell; Krzysztof Matyjaszewski; *Biomacromolecules* **2007,** 8, 1396-1399.
DOI: 10.1021/bm061236j

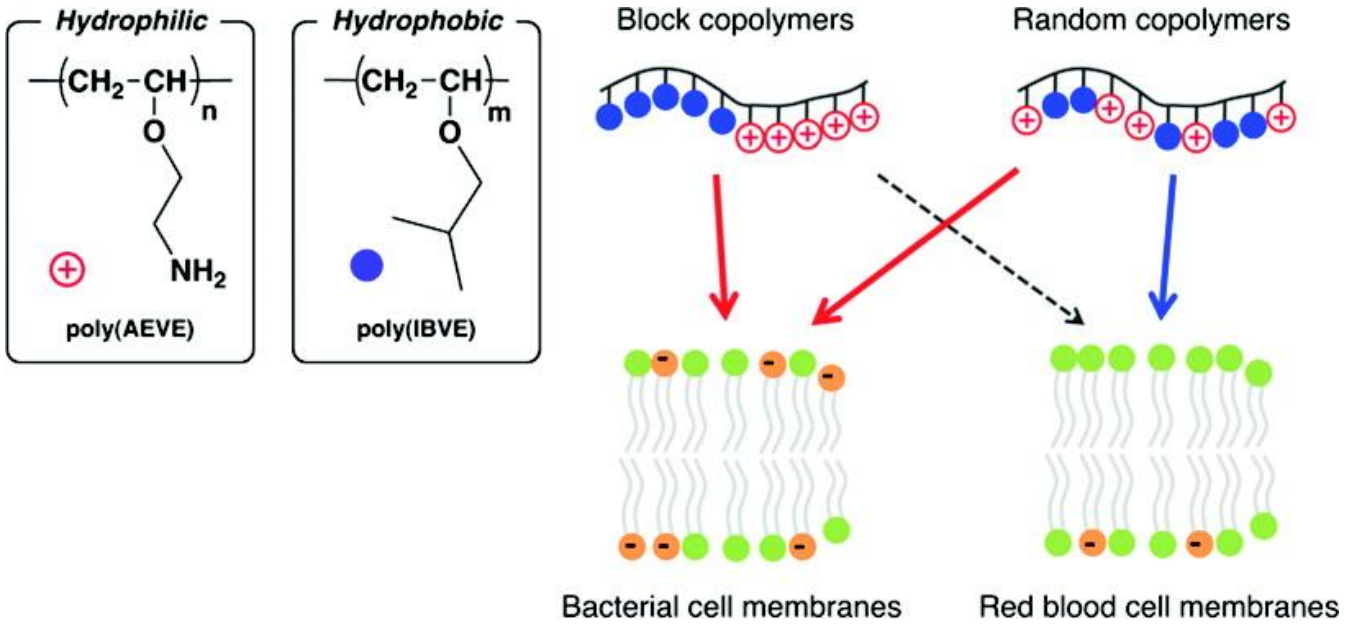


the block copolymers are much less hemolytic compared to the highly hemolytic random copolymers. These results indicate that the amphiphilic copolymer structure is a key determinant of activity

Published in: Yukari Oda; Shokyoku Kanaoka; Takahiro Sato; Sadahito Aoshima; Kenichi Kuroda; *Biomacromolecules* **2011,** 12, 3581-3591.
DOI: 10.1021/bm200780r

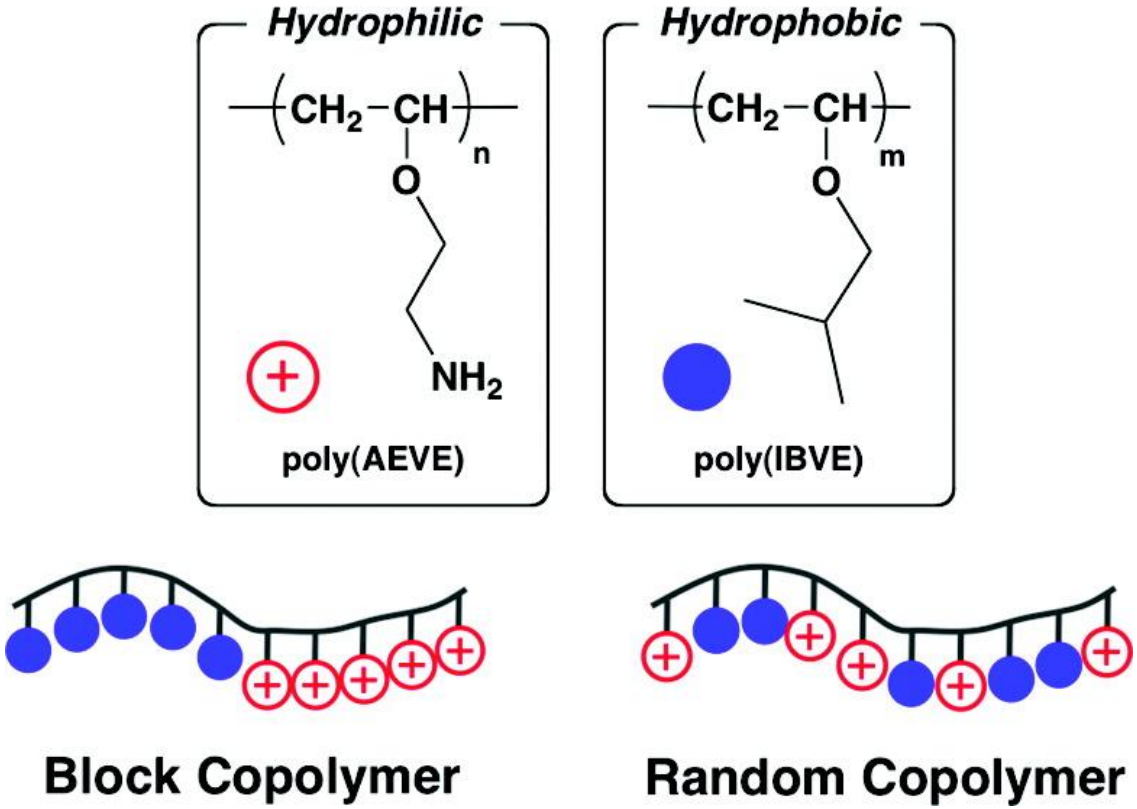


Amphiphilic poly(vinyl ether)s with block and random copolymer structures.

Excess hydrophobicity of polymer chains however, induces their self-association in aqueous media, which would reduce the number of active polymer chains and result in no activity enhancement for polymers with higher compositions of hydrophobic groups

Published in: Yukari Oda; Shokyoku Kanaoka; Takahiro Sato; Sadahito Aoshima; Kenichi Kuroda; *Biomacromolecules* **2011,** 12, 3581-3591.
DOI: 10.1021/bm200780r

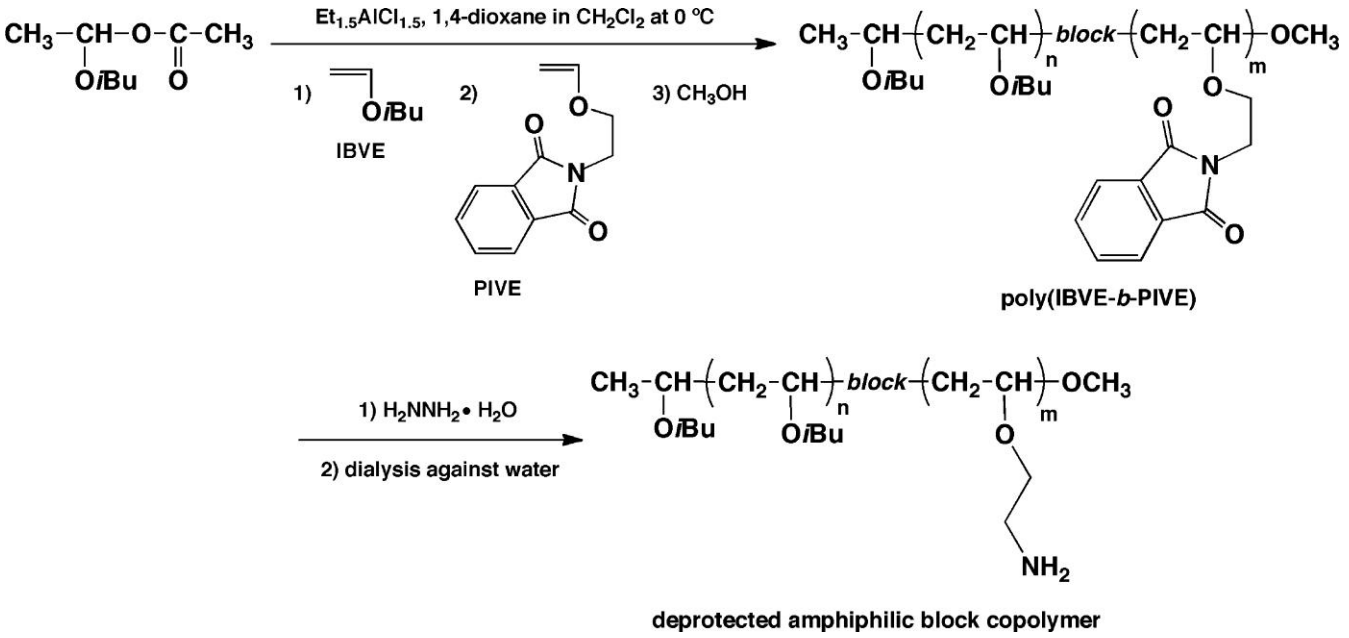


Cationic living polymerization, target is 4000 g/molThe phthalimide protecting groups were removed by treating the polymers with hydrazine, and the crude polymers with primary amine groups were further purified by dialysis against water to remove low MW impurities. $^{1}$H NMR analysis indicated the yield of deprotection was >99%

Published in: Yukari Oda; Shokyoku Kanaoka; Takahiro Sato; Sadahito Aoshima; Kenichi Kuroda; *Biomacromolecules* **2011,** 12, 3581-3591.
DOI: 10.1021/bm200780r

2. $^1$H NMR spectra for precursors of amphiphilic poly(vinyl ether)s and products obtained after deprotection

(A) Homopolymer

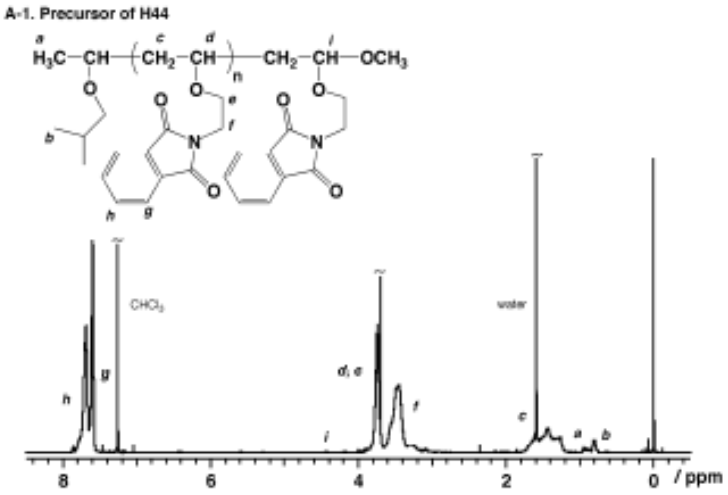


Degree of polymerization (n) was calculated from an integral ratio (*g*, *h*) / (*a*, *b*).

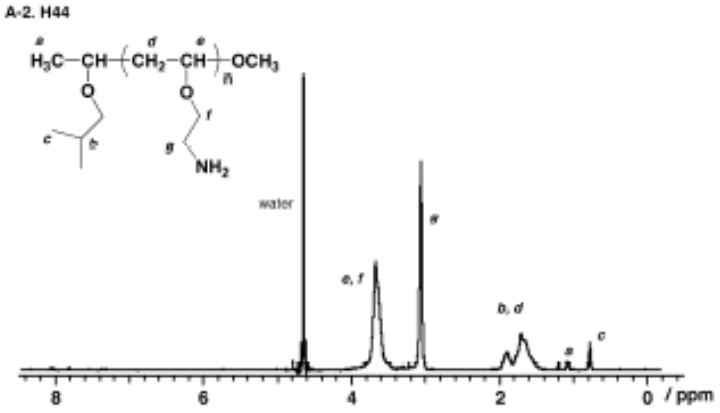


**Figure S2.** $^1$H NMR spectra for the precursor of H44 in $CDCl_3$ (A-1) and H44 in $D_2O$ (A-2).

**1H NMR analysis indicated the yield of deprotection was >99%**

- Preparation of FITC-Labeled Block Copolymer Amphiphilic block copolymer (10 mg, [NH2] = 0.081 mmol) was dissolved in DMF (10 mL) and triethylamine (30 μL, 0.24 mmol). Fluorescein isothiocyanate (FITC, Aldrich) (3.2 mg, 8.1 × 10–3 mmol) in DMF (2 mL) was added into the reaction mixture. The reaction mixture was stirred for 4 h at room temperature in the dark. After the solvent was removed under reduced pressure, the residue was dissolved in methanol. Unreacted FITC was removed by size exclusion chromatography (Sephdex LH-20 gel, Amersham Biosciences, Uppsala, Sweden) using methanol. Comparing the molar absorbance coefficient of F-B3826 and free fluorescein, the average number of FITC molecule per block copolymer chain is 0.45 (Supporting Information). This corresponds to one FITC molecule in 62 amine groups

# protected precursor polymer

| entry | copolymer structure | DP[a] PIVE | DP[a] IBVE | $MP_{IBVE}$[b] (mol %) | $M_n$ (NMR)[c] | $M_w/M_n$ (GPC)[d] | deprotected polymer[e] |
|---|---|---|---|---|---|---|---|
| 1 | homopolymer | 44 (40) | 0 (0) | 0 | 9600 | 1.11 | H44 |
| 2 | random copolymer | 30 (30) | 10 (10) | 25 | 7500 | 1.13 | $R40_{25}$ |
| 3 | | 18 (20) | 20 (20) | 53 | 5900 | 1.14 | $R38_{53}$ |
| 4 | | 8 (10) | 30 (30) | 79 | 4700 | 1.31 | $R38_{79}$ |
| 5 | diblock copolymer | 28 (30) | 10 (10) | 26 | 7100 | 1.16 | $B38_{26}$ |
| 6 | | 19 (20) | 20 (20) | 51 | 6100 | 1.11 | $B39_{51}$ |
| 7 | | 9 (10) | 30 (30) | 77 | 5000 | 1.37 | $B39_{77}$ |
| 8 | | 43 (45) | 15 (15) | 26 | 10800 | 1.19 | $B58_{26}$ |
| 9 | | 58 (60) | 20 (20) | 26 | 14600 | 1.14 | $B78_{26}$ |
| 10 | | 92 (100) | 50 (50) | 35 | 25000 | 1.14 | $B142_{35}$ |

a Calculated by comparing the integral area of signals from the phthalimide group relative to that of the methyl group of the isobutyl group in $^1$H NMR spectra. The theoretical DP based on the feed monomer composition is presented in the parenthe

b Mole percentage of IBVE relative to the total number of monomers in a polymer chain.

c Calculated based on DP and molecular weight of monomeric units.

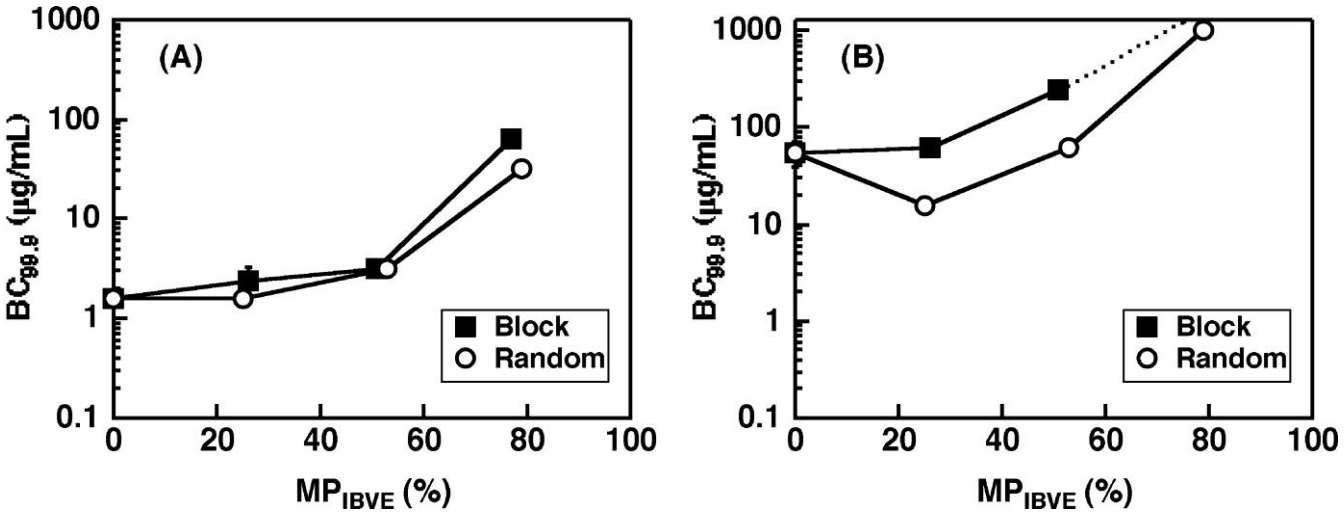


Bactericidal activity (BC99.9) against E. coli of block copolymers (filled squares) and random copolymers (empty circles) with DP ~ 40 as a function of the mole percentage of hydrophobic isobutyl side chains (MPIBVE) in HEPES buffer (A) and MH broth (B). Each data point and error bar represents the average and standard deviation of two independent experiments in duplicate. The BC99.9 value of B3977 in MH broth was over 1000 μg/mL.

The activity reduction by the intramolecular hydrophobic aggregation appears to be more dominant for the random poly(vinyl ether)s than the activity enhancement by hydrophobicity, as found in other polymers. On the other hand, the more rigid polymers (polymethacrylates, polynorbornenes, and polyamides) are likely to have more extended conformations, and the hydrophobic groups would be more exposed to the surrounding aqueous environment. As a result, the more rigid polymers reflect

their hydrophobicity more directly on the membrane disruption action, increasing their antibacterial activity

We further speculated that the decrease in activity of the random poly(vinyl ether)s could be related to the flexible backbone of poly(vinyl ether)s, which would allow the hydrophobic side chains to associate in aqueous solution more easily compared to more rigid polymers. Therefore, the flexible poly(vinyl ether) chains could facilitate the formation of intramolecular aggregates, which reduce the number of active polymer chains against bacteria.

---

Published in: Yukari Oda; Shokyoku Kanaoka; Takahiro Sato; Sadahito Aoshima; Kenichi Kuroda; *Biomacromolecules* **2011,** 12, 3581-3591.
DOI: 10.1021/bm200780r

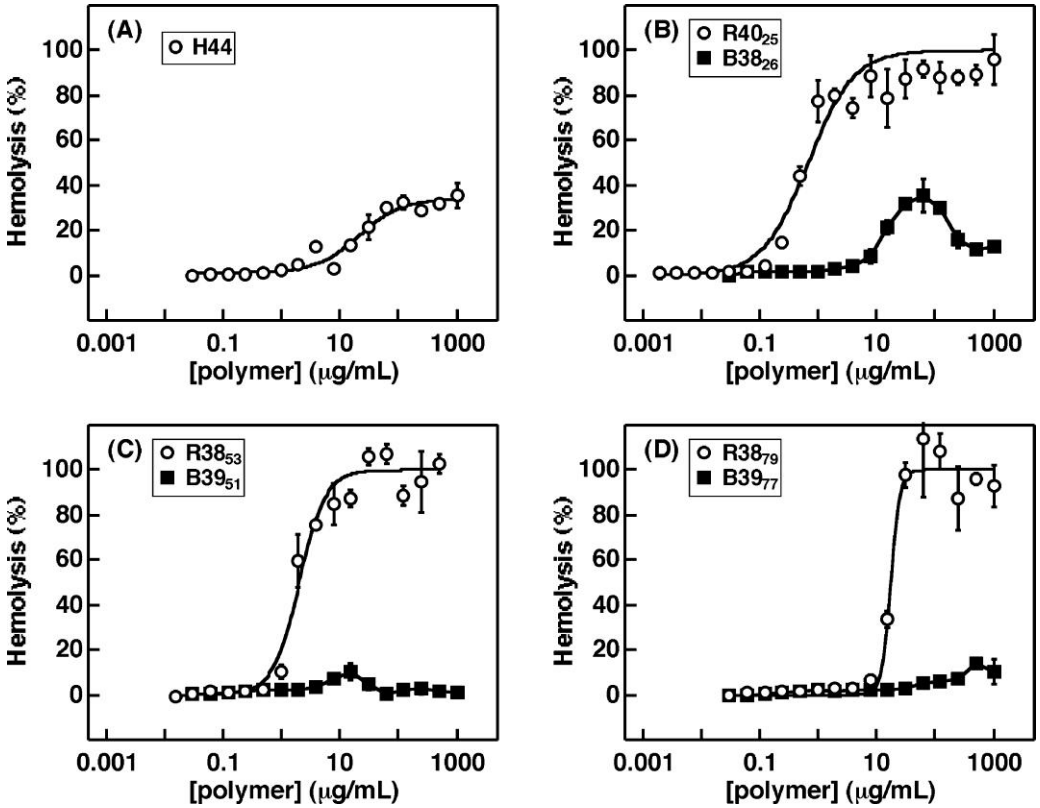


Percentages of hemolysis induced by homopolymer (A), copolymers with MPIBVE = ~25% (B), 50% (C), and 80% (D). The data points and error bars represent the average and standard deviations of a representative measurement in triplicate. The sigmoidal curves of homopolymer (A) and random copolymers (B–D) are best fits to the Hill equation.

The HC50 values of the random copolymers increased with increasing MPIBVE, indicating that increasing the hydrophobicity of polymers reduces the hemolytic activity. However, random amphiphilic polymethacrylates with high mole percentages of hydrophobic side chains showed high hemolytic activity,(11, 15) which is opposite to the results presented in this study. As discussed for the antibacterial activity of polymers, the random poly(vinyl ether)s with higher MPIBVE could form intramolecular aggregates due to the flexible polymer backbone, which reduces the active polymer chains, resulting in the lower hemolytic activity.

Published in: Yukari Oda; Shokyoku Kanaoka; Takahiro Sato; Sadahito Aoshima; Kenichi Kuroda; *Biomacromolecules* **2011,** 12, 3581-3591.
DOI: 10.1021/bm200780r

| | $BC_{99.9}$[a] (μg/mL) | | $HC_{50}$[b] (μg/mL) | $C_H$[d] (μg/mL) |
|---|---|---|---|---|
| **polymer** | **in HEPES** | **in MH broth** | | |
| H44 | 1.6 ± 0.0 | 54.7 ± 15.6 | >1000 (max 42.5 ± 6.3%)[c] | 0.98 |
| $R40_{25}$ | 1.6 ± 0.0 | 15.6 ± 0.0 | 0.49 ± 0.17 | >1000 |
| $R38_{53}$ | 3.1 ± 0.0 | 62.5 ± 0.0 | 1.8 ± 0.24 | >500 |
| $R38_{79}$ | 31.3 ± 0.0 | 1000 ± 0.0 | 18.9 ± 1.3 | >1000 |
| $B38_{26}$ | 2.4 ± 0.91 | 62.5 ± 0.0 | >1000 (max 37.7 ± 2.8%)[c] | 2.0 |
| $B39_{51}$ | 3.1 ± 0.0 | 250 ± 0.0 | >1000 (max 12.9 ± 6.3%)[c] | 0.49 |
| $B39_{77}$ | 62.5 ± 0.0 | >1000 | >1000 (max 22.8 ± 8.5%)[c] | 0.78 |

a Determined in HEPES buffer or MH broth against *E. coli*.
b The $HC_{50}$ values and errors were reported as average and standard deviations of the three independent experiments, respectively.
c Local maximum values of hemolysis induced by each polymer.
d The lowest polymer concentration to induce hemagglutination.

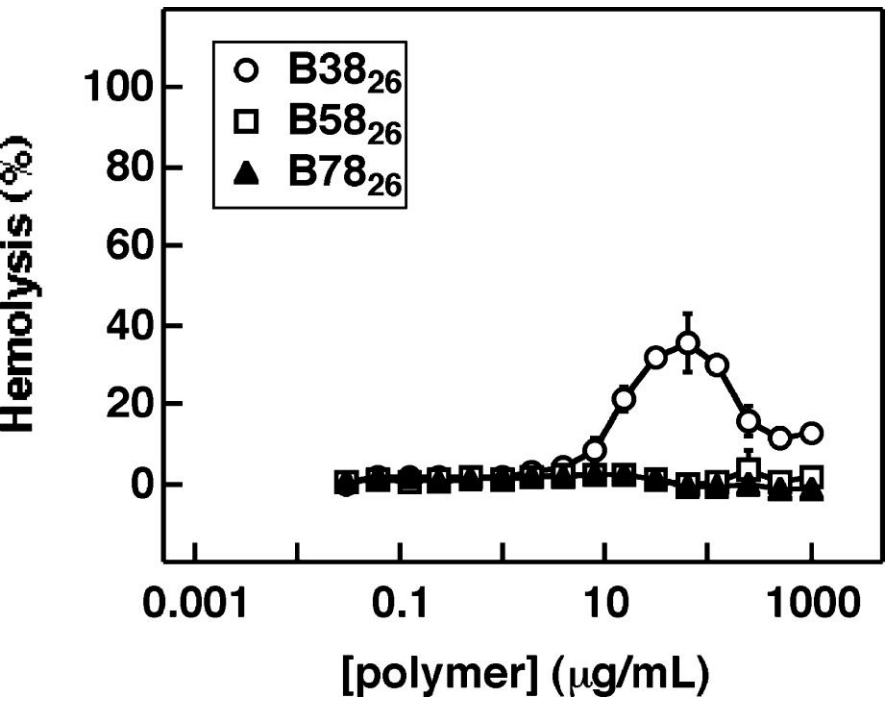


Table 3. Effect of Polymer Length on Bactericidal Activity of Block Copolym

| | $BC_{99.9}$[a] | | | |
|---|---|---|---|---|
| | in HEPES | | in MH broth | |
| polymer | (μg/mL) | (μM) | (μg/mL) | (μM) |
| $B38_{26}$ | 2.4 | 0.66 | 62.5 | 17.5 |
| $B58_{26}$ | 0.78 | 0.15 | 62.5 | 11.9 |
| $B78_{26}$ | 1.6 | 0.22 | 31.3 | 4.4 |

a Determined in HEPES buffer or MH broth against *E. coli*.

Percentages of hemolysis induced by B3826 (empty circles), B5826 (empty squares), and B7826 (filled triangles) as a function of polymer concentration. Error bars represent the standard deviations from triplicate measurements. B3826 caused a local maximum of 30% hemolysis at 100 μg/mL, but the block polymers with increased DP, B5826, and B7826, induced no hemolysis up to 1000 μg/mL. This indicates that the hemolytic activity of the block copolymers was reduced by increasing the DP.

Published in: Yukari Oda; Shokyoku Kanaoka; Takahiro Sato; Sadahito Aoshima; Kenichi Kuroda; *Biomacromolecules* **2011,** 12, 3581-3591.
DOI: 10.1021/bm200780r

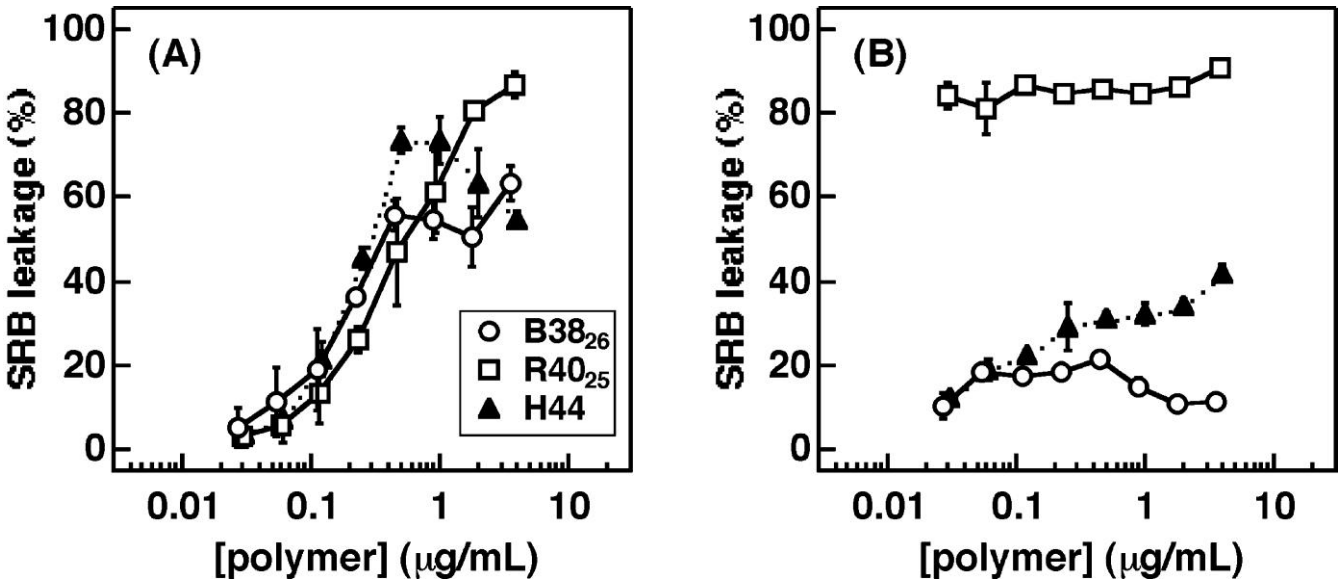


Percentages of SRB leakage from LUVs composed of (A) POPE/POPG (4:1) and (B) eggPC. The LUVs were incubated with the polymers B3826 (empty circles), R4025 (empty squares), and H44 (filled triangles) at 37 ° C for 1 h. The error bars represent the standard deviations from triplicate measurement.

LUVs with POPE/POPG (4:1) and eggPC are simplified model membranes of the *E. coli* and RBC cell membranes, respectively. These model vesicles are limited by their lipid compositions, as the bacterial cell and RBC membranes are a complex of proteins, lipids, and polysaccharides on the cell surface with membrane asymmetry. The leakage from eggPC LUVs depended on the amphiphilic copolymer structures (Figure 5B). The leakage induced by the block copolymer $B38_{26}$ was lower than 20% although the random copolymer $R40_{25}$ induced >80% leakage in the entire concentration range (0.029–3.8 μg/mL). These results suggest that the block copolymer selectively disrupts the bacteria-type membranes over the erythrocyte-type membranes, which appears to reflect the selective activity of polymers against *E. coli* over RBCs although the antibacterial actions of polymers remain unclear.

Published in: Yukari Oda; Shokyoku Kanaoka; Takahiro Sato; Sadahito Aoshima; Kenichi Kuroda; *Biomacromolecules* **2011,** 12, 3581-3591.
DOI: 10.1021/bm200780r

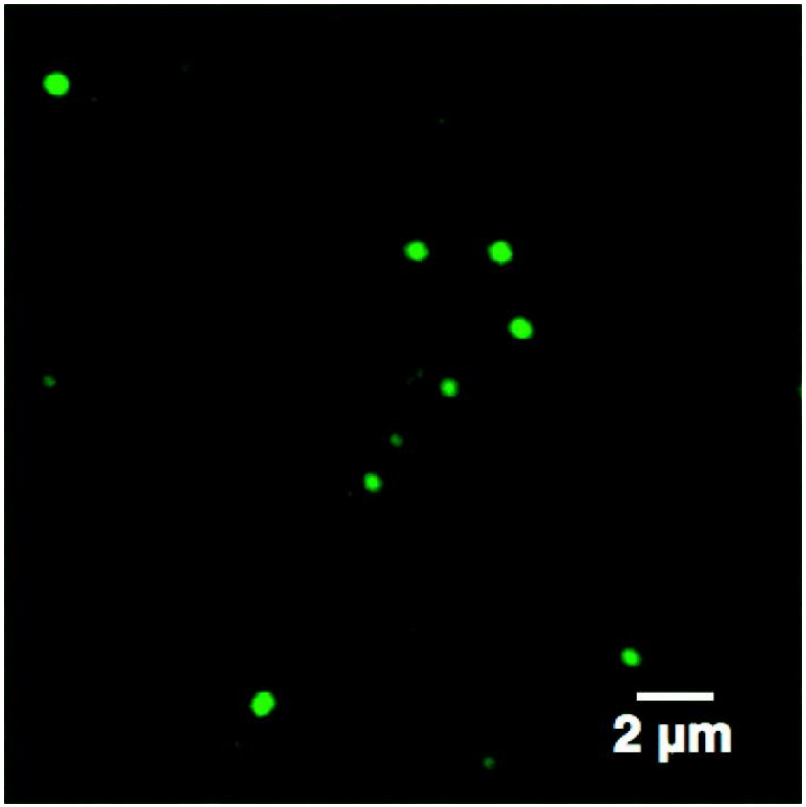


Confocal fluorescent microscopy image (single layer image) of 50 µg/mL B3826 containing F-B3826 in HEPES buffer (1% v/v DMSO; FITC: 5.3 mol % relative to the total number (mole) of B3826 polymer chains).

Published in: Yukari Oda; Shokyoku Kanaoka; Takahiro Sato; Sadahito Aoshima; Kenichi Kuroda; *Biomacromolecules* **2011,** 12, 3581-3591.
DOI: 10.1021/bm200780r

# Table 4. Characterization of Polymer Aggregates in HEPES Buffer

| polymer | $S^2_{z}^{1/2}$ [a] (nm) | $R_H$ [b] (nm) | $M_w$ [c] | $N_{agg}$ [d] | CAC [e] (μg/mL) | $BC_{99.9}$ [f] (μg/mL) | $HC_{50}$ (μg/mL) |
|---|---|---|---|---|---|---|---|
| B38<sub>26</sub> | 200 | 250 | $8.1 \times 10^7$ | 20000 | 36 | 2.4 ± 0.91 | >1000 |
| R40<sub>25</sub> | 27 | n.d. [g] | $9.4 \times 10^4$ | 22 | 380 | 1.6 ± 0.0 | 0.49 ± 0.17 |

a Radius of gyration, determined by SLS.
b Hydrodynamic radius, determined by DLS.
c Weight-average molecular mass, determined by SLS.
d Aggregation number, calculated from the weight-average molecular weight of polymer chain and $M_w$.
e Critical (intermolecular) aggregation concentration, determined by SLS.
f Determined in HEPES buffer.
g The scattering intensities were too low to obtain accurate autocorrelation functions.

3. Determination of the critical (intermolecular) aggregation concentration (CAC)

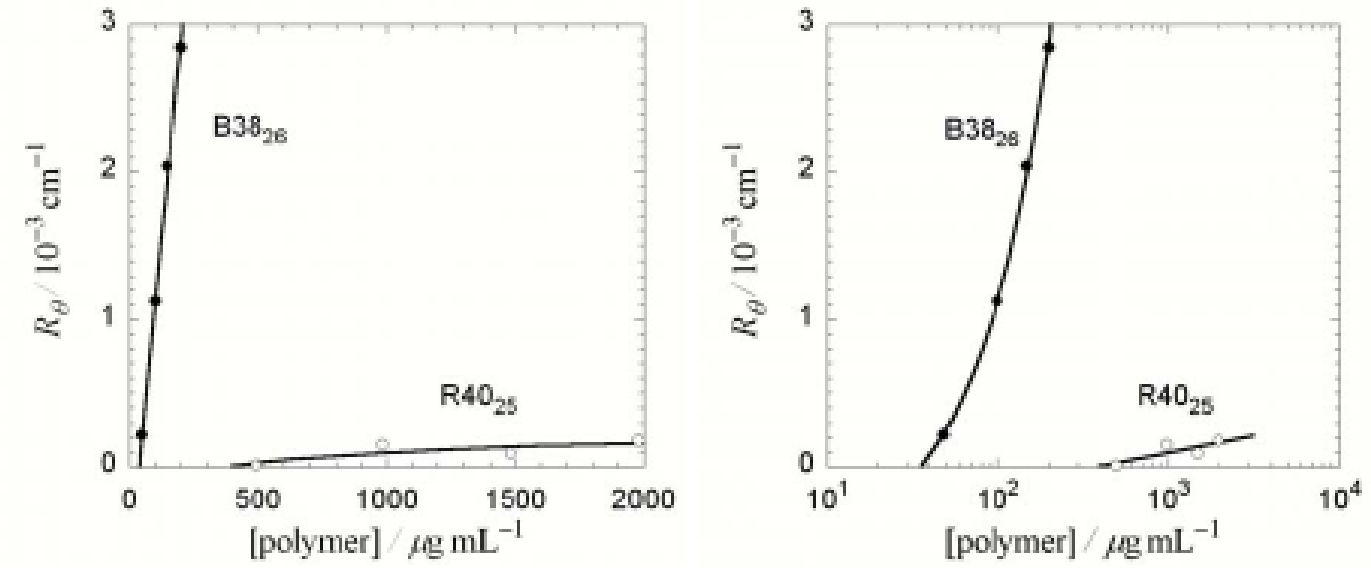


**Figure S7.** Linear (left) and semi-logarithmic (right) plots of the excess Rayleigh ratio against the polymer concentration for aqueous solutions of samples $B38_{26}$ and $R40_{25}$.

The critical (intermolecular) aggregation concentration (CAC) was determined as the polymer concentration where the excess Rayleigh ratio $R_\theta$ becomes infinitely low. Figure S7 shows the polymer concentration dependence of $R_\theta$ at $\theta = 30°$ for aqueous solutions of samples $B38_{26}$ and $R40_{25}$, from which CAC were determined to be 36 μg/mL and 380 μg/mL for $B38_{26}$ and $R40_{25}$, respectively.

4. Static and dynamic light scattering data

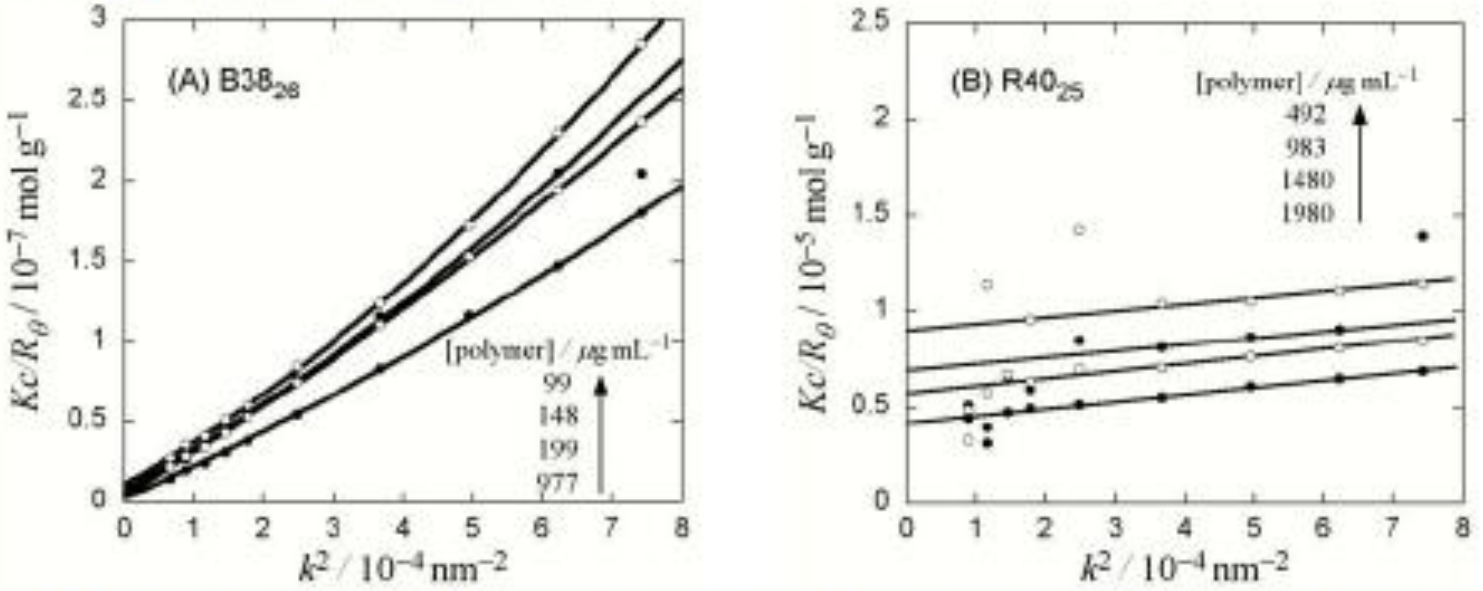


Figure S8. Static light scattering (SLS) results for B38$_{26}$ (A) and R40$_{25}$ (B) in HEPES buffer at 37 °C.

The hydrodynamic radius of the block copolymer aggregate obtained by DLS was as large as 250 nm. The aggregate sizes estimated by the light scattering experiments are consistent with those found in the fluorescence image. On the other hand, light scattering intensities from aqueous solutions of the random copolymer R4025 were much weaker than B3826 solutions, and the radius of gyration and the aggregation number were 27 nm and 22, respectively, in the copolymer concentration range 500–2000 μg/mL

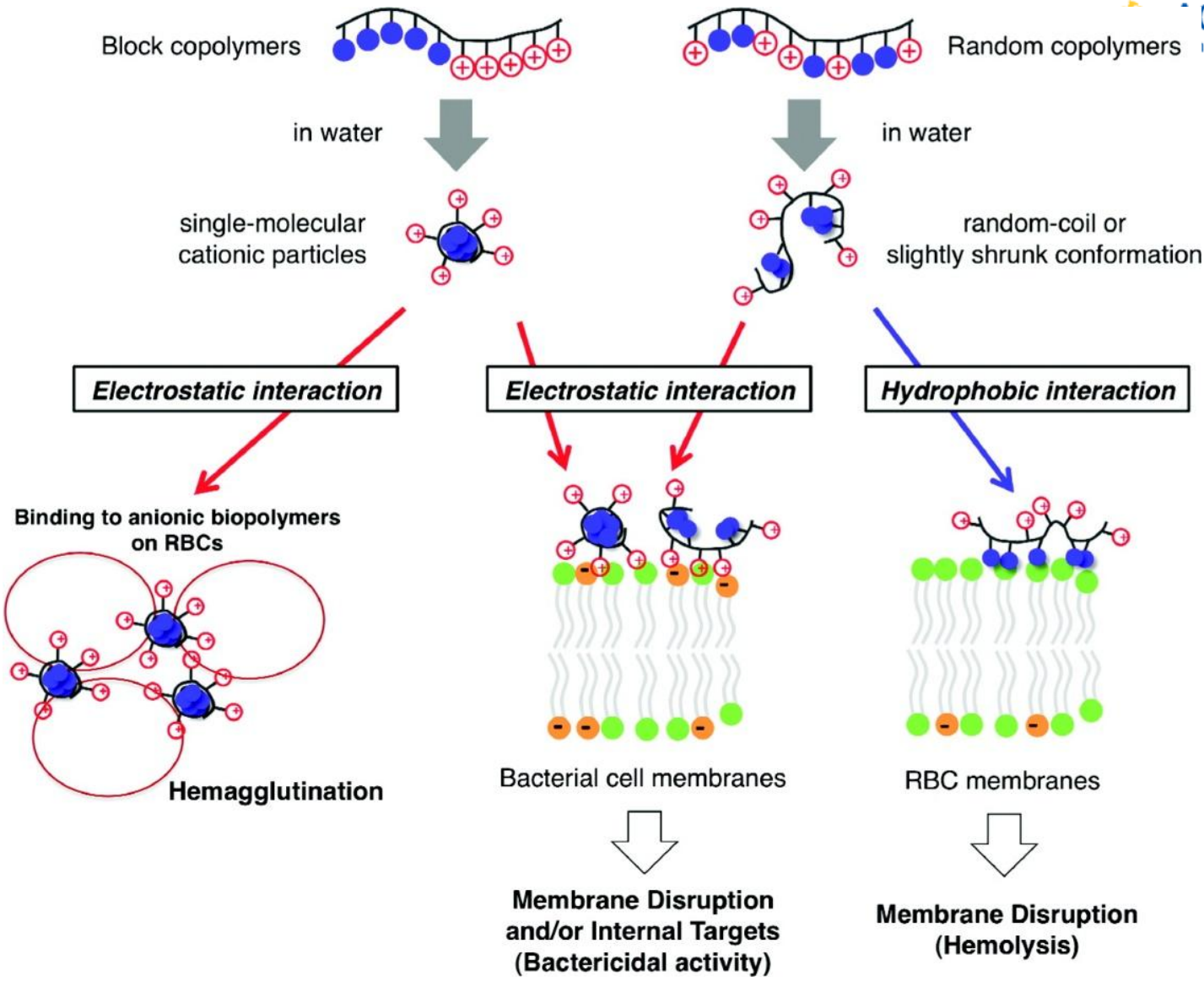


Schematic presentation of proposed antibacterial and hemolytic activities.

Published in: Yukari Oda; Shokyoku Kanaoka; Takahiro Sato; Sadahito Aoshima; Kenichi Kuroda; *Biomacromolecules* **2011,** 12, 3581-3591.
DOI: 10.1021/bm200780r

The block copolymers could form intramolecular aggregates with a hydrophobic core wrapped by the cationic segment in water, which can be regarded as single-molecular cationic particles. The cationic properties of these intramolecular aggregates would increase their electrostatic binding to anionic lipopolysaccharides (LPS) on the *E. coli* cell surface and may replace the divalent cations, which stabilize the outer membrane structure. The replacement of these divalent cations destabilizes the membrane structure and increases permeability of the outer membrane, which would promote uptake of the polymers into the cell surfaces as found in antimicrobial peptides. The polymers could diffuse through the peptidoglycan layer to reach cytoplasmic membranes with anionic lipids and cause membrane disruption, leading to lethal leakage of cellular contents. The cationic groups of polymers could induce the segregation of anionic lipids or cause strong perturbation of the cell wall integrity.Alternatively, the polymers might transit the cytoplasmic membrane and interact with potential targets in the cytoplasma, inhibiting macromolecular synthesis as found for some antimicrobial peptides. As for the hemolytic activity, the hydrophobic segment is shielded by the cationic surfaces, reducing the hydrophobic binding of polymers to the cell membranes of RBCs, thus, causing no significant hemolytic activity. However, the high cationic charge density of the intramolecular aggregates could interact strongly with the anionic biopolymers on the RBC surfaces, which cause hemagglutination. On the other hand, random copolymers would take a random-coil or slightly shrunk conformation because the hydrophobic groups randomly distributed along the polymer chain may not form the hydrophobic core (Figure 7), if the hydrophobic content is low enough